Article

Climate Impact and Model Approaches of Blue-Green Infrastructure Measures for Neighborhood Planning

Maike Beier [1,*], Jessica Gerstendörfer [1], Katja Mendzigall [2], Dirk Pavlik [2], Peter Trute [2] and Robert von Tils [2]

1 Institute of Sanitary Engineering and Waste Management, Leibniz University Hannover, 30167 Hannover, Germany; gerstendoerfer@isah.uni-hannover.de
2 GEO-NET, 30161 Hannover, Germany; mendzigall@geo-net.de (K.M.); pavlik@geo-net.de (D.P.); trute@geo-net.de (P.T.); rvontils@geo-net.de (R.v.T.)
* Correspondence: beier@isah.uni-hannover.de

Abstract: Nowadays, most cities deal with the problem of "Urban Heat Islands". Especially existing city districts cannot easily be adapted. In this paper, the effects of blue-green infrastructure elements (BGI) on air and surface temperature in courtyards are examined, based on on-site measurements and simulations. Recognizable effects on the temperature were observed: BGI lower the number of hot days in the courtyard, including a faster air temperature drop at night, but water elements increase the number of tropical nights due to their heat capacity. Model simulations with PALM-4U proved to be useful to analyze the effects of BGI on the microclimate. Besides analyzing existing structures, the effects of planned measures can be quantified by simulation. However, for this application, needs of improvement were recognized to evaluate the influence of BGI on the microclimate more realistically. For decision support, standard indicators such as the number of tropical nights and hot days are not differentiated enough to quantify specific climate stress of urban residents. It is suggested to consider summer days additionally, percentiles could be used instead of fixed thresholds and the entire course of the year should play a role in the evaluation of the elements and urban design.

Keywords: urban microclimate; PALM; inner courtyards; thermal stress; decision support

1. Introduction

Heat stress puts an enormous strain on human health and leads to many deaths caused by increasingly frequent heat waves [1–5]. At the same time, the quality of the living environment of the quarters is decisively affected by the implementation of blue-green infrastructure elements. Many authors clearly state the correlation between air temperatures and mortality [6,7]. Beside deaths, also heat-related diseases like heat stroke [8] have to be considered. In particular, summer heat waves with several successive tropical nights are an additional burden for the elderly, children, and the chronically ill [1,2] and for the future climate change will further increase the duration and intensity of heat waves.

Due to the high number of sealed surfaces that lead to the absorption of solar radiation, dense buildings, little greenery and poor air circulation in urban areas [8], cities often have higher air temperatures, especially during the night, than rural areas. This effect is referred to as the "urban heat island" [8–12] and the municipalities worldwide are trying to address this problem through appropriate infrastructural measures. In addition to heat stress, dealing with heavy rainfall events is also one of the challenges cities face in adapting to climate change, as these have become more frequent in recent years [13,14] and often lead to flooding as well as combined sewer overflows, especially in existing neighbourhoods, resulting in ecological and economic damage [15–17]. In order to achieve sustainability goals such as resilience, climate adaptation and environmental protection, strategies for urban areas are needed and many German cities prepare climate adaption strategies to counteract these problems [18,19].

Currently, the topic of heat adaptation and urban water management is increasingly dealt with in an integrative way in the environmental planning process. Within the framework of the research project "TransMiT", which is oriented towards a climate adapted urban development and water management in the long term, methodological and substantive approaches are addressed, through which the climate impact of blue-green infrastructure can be determined and evaluated. Figure 1 shows where the research is to be placed, i.e., to prove a modelling attempt for decision support at the level of strategic planning for urban districts comparing the effects of one specific LID element (ponds) for one typical urban structure (closed courtyard). While climate models usually are used to evaluate whole city areas, focuses this paper on a smaller resolution (courtyard). Furthermore, the attempt was made modelling overall effects (greenings plus water elements) instead of considering small individual effects.
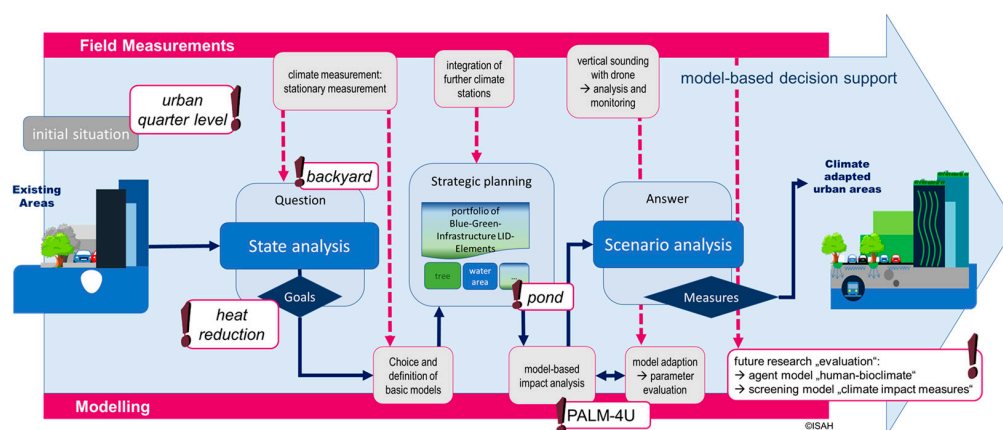

Figure 1. Schematic diagram showing the interaction of measurements and modelling in model-based planning—including the different methods used in the study (gray background) and specific research items selected to exemplify the methods (pink framed fields with exclamation marks).

Storm water management measures offer a great potential of synergy effects concerning local heat management with the blue-green infrastructures (BGI) located in the urban areas to decouple and delay runoff.

As pointed out in [20], heat mitigation by green courtyards is well documented (see [21]), However, gaps exist in the microclimatic effects of blue elements, such as open cisterns and ponds. Therefore, special attention was given to determine synergies of the BGI elements for the courtyard on their individual effects on the microclimate during heat waves. Within this study, the question whether ponds are suitable to reduce the (nocturnal) overheating in the neighborhoods is discussed beside the methodology approach analyzing differently equipped courtyard situations:

a. an inner courtyard in the Südstadt district of Hannover, where blue elements (ponds and cisterns) and various greening measures were implemented in 2019 (so-called "Blue Courtyard").

b. In comparison, measurements were conducted at a courtyard in Hannover Linden, which was only equipped with green elements (referred to as the "green courtyard").

The aim was to achieve statements on the effectiveness of the BGI measures based on stationary climate measurements in the courtyard situation and their integration into a network of further climate stations (DWD). These comparisons are supplemented and extended by vertical soundings of the temperature situation with the help of drone ascents. In a further analysis step, the PALM-4U microscale climate model is applied to simulate the high spatial resolution temperature fields for the courtyard situations. In future, dynamic model approaches for climate-ecological impact analysis (=(climate) agent model) are to be implemented on this data basis, or simplified screening approaches for climate impact oriented to planning practice are to be derived.

2. Materials and Methods

2.1. Observation Area

The study was carried out in Hannover, Germany, located in Lower Saxony. The city of Hannover has around 534,000 inhabitants (June 2020, [22]) and a land area of around 204 km^2. 35.9% of the area are built up, 15.2% are roads, squares and paths, 7.8% are green spaces, agricultural and horticultural land account to 17.2%, 13.2% are forests and woods, 3.5% are water bodies [23].

As part of a cooperation project between the German Meteorological Service (DWD) and the city of Hannover, three temporary measuring stations were set up in Hannover to record the heat island effect in addition to the official DWD measuring station at the airport (ID 2014), with the inner-city area being recorded in comparison to the outskirts of the city [24]. The results show a significant difference between inner-city stations and the outskirts stations, especially concerning tropical nights. Moreover, to capture the large spatial variability of air temperature within urban structures, mobile measurements were carried out by the DWD during a heat phase in the summers of 2018 and 2019 with a measurement vehicle. The results shown in [24] emphasize the cooling effect of the city forest "Eilenriede" and the "Leine"-floodplain and "Maschsee"-lake while also in contrast the heating effect of the built-up areas. A climate adaptation map as part of Hannovers climate change adaptation strategy addresses these cooling and heating effects and identifies critical inner-city areas (cf. [25]). In the presented study, three different courtyards located in the inner-city area are observed. Table 1 summarizes the properties of the courtyards and highlights the differences in their design and the particular research/measurement focus. In the Appendix A, the courtyards are described in detail (see Appendix A).

Table 1. Main characteristics of the observed courtyards.

Information	Courtyard 1	Courtyard 2	Courtyard 3
Designation	"blue courtyard"	"comparison courtyard"	"green courtyard"
Owner	Housing cooperative Gartenheim eG	Trust GmbH Wedemeier Treuhand	Housing cooperative spar + bau
Location	Hannover Südstadt	Hannover Südstadt	Hannover Linden
Size	~3652.10 m^2	~3696 m^2	~3700 m^2
BGI Specification	**Blue elements** • pond 1: 140 m^2 surface (according to plan), deepest point 45 cm • pond 2: 70 m^2 surface (according to plan), deepest point 110 cm • water volume both ponds together ca. 50 m^3; • 3 cascade systems à 3 open cisterns, 0.64 m^2, 40 cm depth, 235 L **Green elements** • Trees, bushes • Few lawn areas (Figure A4) **other elements** • Playground (sand) • Pavements (gravel)	No blue elements **Green elements** • Hedges, trees • Lawn areas **other elements** • water playground (sand, stone material)	No blue elements **Green elements** • Raised garden beds → 4 corners of the courtyard à 6 beds on sealed ground, 160 m^2 • Hedges, 5 trees in the middle • Large lawn area, dominating the courtyard (see Appendix A) **other elements** • pavements (concrete, stone material)
Evaluation	weather station drone measurement Simulation	- - Simulation	- drone measurement -

2.2. Weather Stations

　　Data from several weather stations belonging to the DWD (German Meteorological Service) in the city of Hannover and the surrounding area (airport) were evaluated to compare the temperature trends. The weather station at the airport is installed permanently (ID 2014) while the weather stations at *Weidendamm* (WD), *Marianne-Baecker-Allee* (MBA) and *Kattenbrookspark* (KP) were mobile stations from another research project (see [25], data provided by DWD, Regional Climate Office Hamburg) as the data from IMuK (measurement tower, see Appendix C). Figure 2 shows all mentioned weather stations, while Appendix B gives more details about the stations. As temporal resolution, 10-min data were used, i.e., maximum value or minimum value of 10-min periods. The possibility that the weather station measurements presented in this paper are influenced by shading, direct solar radiation, or precipitation during the measurements cannot be excluded. These effects could lead to falsified results.

Figure 2. Approximate location of the different weather stations within the city of Hanover on a Google Maps screenshot (adapted, map data © 2022 GeoBasis-DE/BKG © 2022, Google, usage with permission according general guidelines by Google and the fair use copyright). The vertical scale is around 18 km and the horizontal scale 17 km.

2.3. Drone Measurement

Drone measurements were carried out by IMuK on the 17 June 2020 in the blue courtyard and on 31 July 2020 in the green courtyard on a cloudless sunny day at midday (autochthonous weather) as punctual measurements. The drone measurements consisted of two parts. One part was an observation of the courtyards with an infrared camera (Figure 3b) and the second part was a vertical probing (Figure 3a) up to 100 m to create a vertical profile for air temperature (and potential temperature respectively), humidity, wind direction and wind velocity. Although both measurements took place on different days, the weather conditions and measurement times were chosen to comparable to a large extent (e.g., level of clouds, point of time, solar radiation, no shading).

(**a**)   (**b**)

Figure 3. Drones from IMuK for measurements in the green and blue courtyard (**a**) for vertical probing and (**b**) for infrared measurements.

2.4. PALM-4U Model Description

PALM is a parallelized large eddy simulation model that has been continuously developed at the Institute for Meteorology and Climatology at the Leibniz Universität Hannover, Germany, since 1997. It serves to investigate micro- and mesoscale turbulent boundary layer flows in the atmosphere and ocean. PALM is optimized for high performance on all types of state-of-the-art processor architectures and scaling up to multiple thousands of processors. It is free to use for research and commercial purposes. As part of the research project [UC]^2—Urban Climate Under Change [26] PALM was further developed into PALM-4U, a model for modeling urban climate issues [27]. A variety of new components have been developed and added to the model. These include, for example, a land surface model, a building surface model, an indoor model, a module for calculating bioclimatic indices, a multi-agent model, and a model for the calculation of the distribution and deposition of air pollutants. PALM-4U is therefore ideally suited to analyze atmospheric processes in urban environments from individual buildings, courtyards and street canyons up to entire cities.

A large number of different urban use cases have been modeled with PALM-4U within the framework of [UC]^2 and also by orders from the administration of various cities. The applicability of PALM-4U for urban climate issues has already been demonstrated many times, although the official validation of the model by the [UC]^2 sub-project "3DO-M" has not yet been fully completed.

In PALM-4U there are two different approaches to simulate turbulent flows: Reynolds-Averaged Navier-Stokes (RANS) and Large Eddy Simulation (LES).

The RANS approach is based on a Reynolds averaging of the Navier-Stokes equations, so that only the development of the ensemble mean over time is considered. Due to the

averaging and the non-linearity of the Navier-Stokes equations exist terms containing turbulent quantities. These terms are replaced by suitable parameterizations.

With LES, the larger-scale energy-carrying vortices are explicitly resolved, whereas the small-scale low-energy vortices (subscales) are parameterized. LES models, compared to RANS models, depend less on parameterizations, since only the part of the turbulence spectrum must be modeled that is smaller than a cut-off length. Because of the universal properties of the small scales, they can be described much easier.

PALM-4U calculates the surface temperature and heat flux of green and non-green ground and building surfaces. Trees are considered with a three-dimensional resolution via a leaf area density (LAD). Water surfaces are currently associated with a temporally constant surface temperature, water bodies are not modeled as PALM-4U does not yet include a water balance model.

2.4.1. Input Data

Climate models need information of the earth surface properties depending on the scale. Urban climate models (UCMs) are developed for applications in a range from mesoscale (up to 50 m grid size) to microscale (up to 1m grid size). The higher the spatial resolution, the more comprehensive and detailed input data are required. PALM-4U is a building resolving model designed for applications on the microscale and requires the following types of input data:

- elevation
- surface layer properties (vegetation, pavement, water)
- buildings (footprint and height)
- soil
- 3D vegetation (optional)
- 3D buildings (optional)

PALM-4U offers the possibility to use three-dimensional building and vegetation structures as input, which were used in this study. This allows, for example, a relatively realistic depiction of the radiative transfer and the flow.

Input data collection and data pre-processing for PALM-4U is a quite extensive process due to different data sources and spatial data formats. A workflow developed at GEO-NET where all collected input data are pre-processed with a Geographical Information System (GIS) and stored in a database was used. The land surface classification for the simulation of the investigation area in Hanover Südstadt is shown in Figure 4. An external script written in R scripting language was used to convert the data from the database into the required input data format of the model. For these first simulations, it was possible to gain all input data from freely accessible sources.
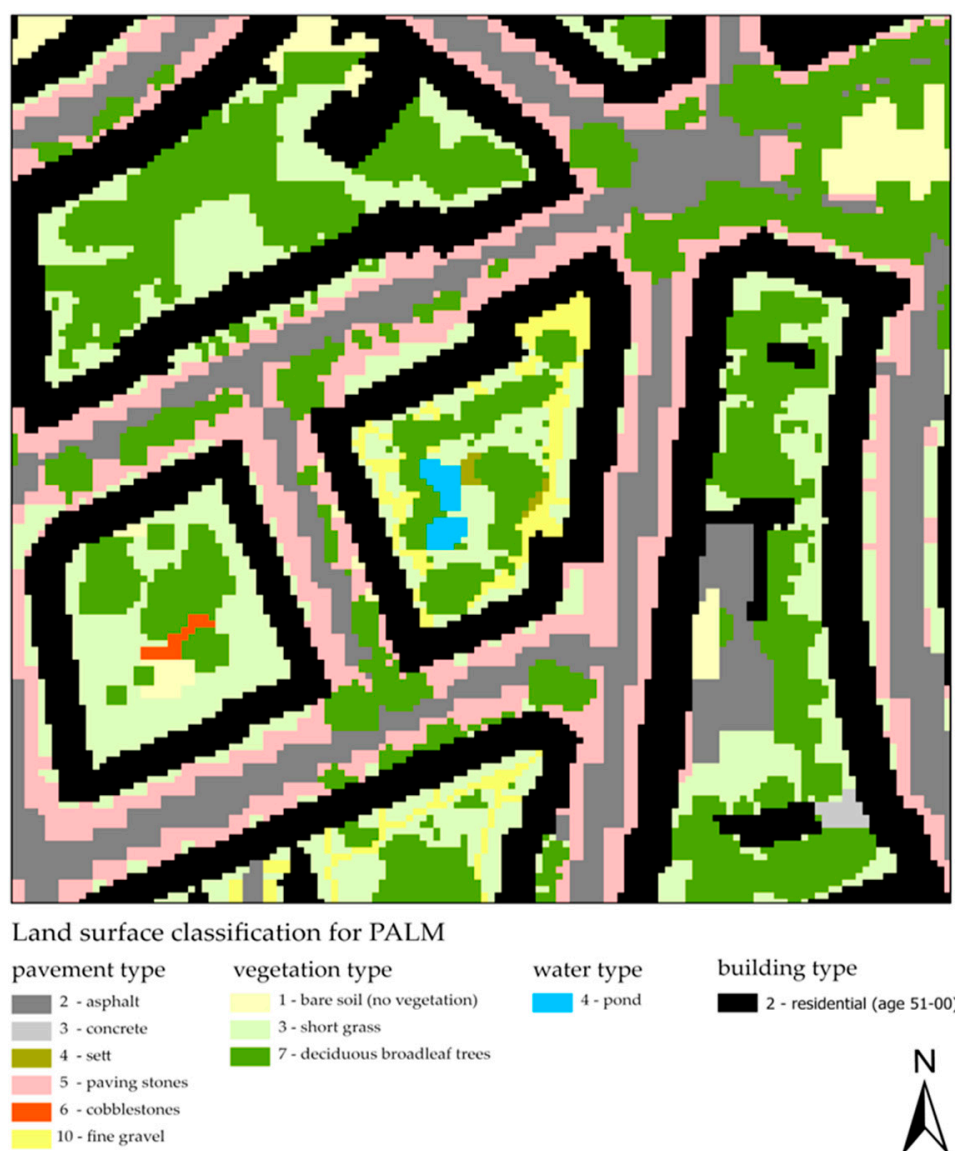
Figure 4. Land surface classification with colored types of pavement, vegetation, water and buildings for the investigation area of the courtyard in Hannover Südstadt.

2.4.2. Model Setup

PALM-4U has many setting options due to the natural complexity of a climate model. For the evaluation of thermal conditions, a standard setup designed was chosen. The model domain has a size of 276 m × 276 m and corresponds to a grid size of 138 × 138 grid points with a horizontal resolution of 2 m.

To match the meteorological conditions of the day the drone measurements took place (17 June 2020), the initial temperature was set to 16.1 °C (289.25 K) and the initial specific humidity was set to 0.001807 kg/kg (which corresponds to nearly 95% relative humidity) at 00:00 UTC +2. Wind was initially set as a light breeze from northwest (315°) with a wind speed of 0.5 m/s.

Start date and time have been set to June 17 at 00:00 UTC +2, with a simulation duration of 40 h. The simulation starts with a spin-up routine which was set to run for 24 h, which, by the experience so far through various simulations with PALM(-4U), is a sufficient amount of time. The spin-up mechanism allows for the adjustment of the inert soil- and wall-layer temperatures to the prevailing atmospheric conditions, prior to the actual atmosphere simulation. An output interval of 15 min instant values and 60 min of time averaged values was chosen.

The model was initiated with cyclic boundary conditions in RANS-mode. The authors are aware that the RANS mode in PALM-4U has not been tested sufficiently yet. The here presented model approach is therefore to be regarded as experimental. The reason for this is that the domain size can be significantly smaller than in LES mode, where the vortex structures of the eddies require a sufficient spatial extent to resolve them completely in space. In the presented case, the demand for computing capacity in RANS mode was therefore significantly lower due to the smaller domain size.

3. Results

For the identification of the specific impact of the BGI, data analysis started identifying hot days and tropical nights at the different weather stations and compare them with the number in the blue courtyard.

3.1. Hot Days

Following the definition of [28] "[...] a day when the maximum air temperature is ≥30 °C", the maxima of the last 10 min of each hour were used for data analysis. As described in [29], based on the German Climate Atlas, the relevant period for hot days is from June to August. However, departing from this, there were hot days and nights in Hanover in September 2020 as well, so that the period under observation was extended from June to September in this study. Figure 5 shows the maximum temperatures per day from 1 June 2020 to 30 September 2020 in comparison for each observed station. It is shown that there was a heat wave between 6–13 August, where each day had an air temperature above 30 °C. According to [30], "a heat wave is a period of several days with unusually high thermal load", but there would be no international consistent definition.
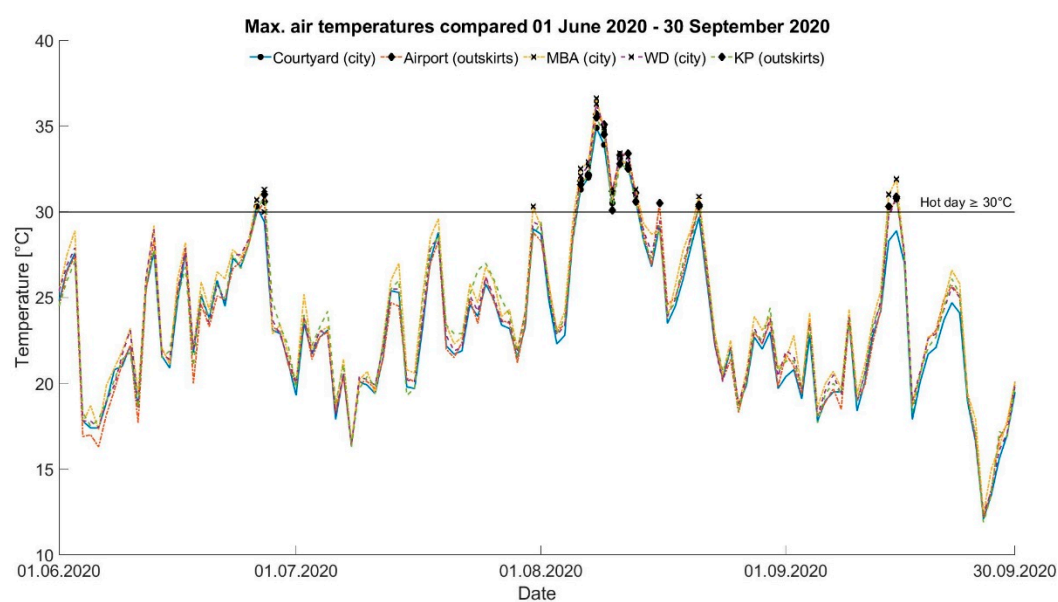

Figure 5. Maximum air temperatures per day from 1 June 2020 to 30 September 2020 for the DWD weather stations at airport, Marianne-Baecker-Allee (MBA), Weidendamm (WD), Kattenbrookspark (KP) and the TransMiT weather station in the blue courtyard. The horizontal line marks the 30 °C limit.

Figure 6 represents the above-mentioned heat wave in detail to show the differences between each weather station clearly. It is obvious that the courtyard's temperatures are the lowest for the first four days of the period, including the two warmest days, but from day five, the KP station shows the lowest temperatures. Tables 2 and 3 summarize the detailed temperatures and give information about the deviations between the DWD stations and the courtyard stations.
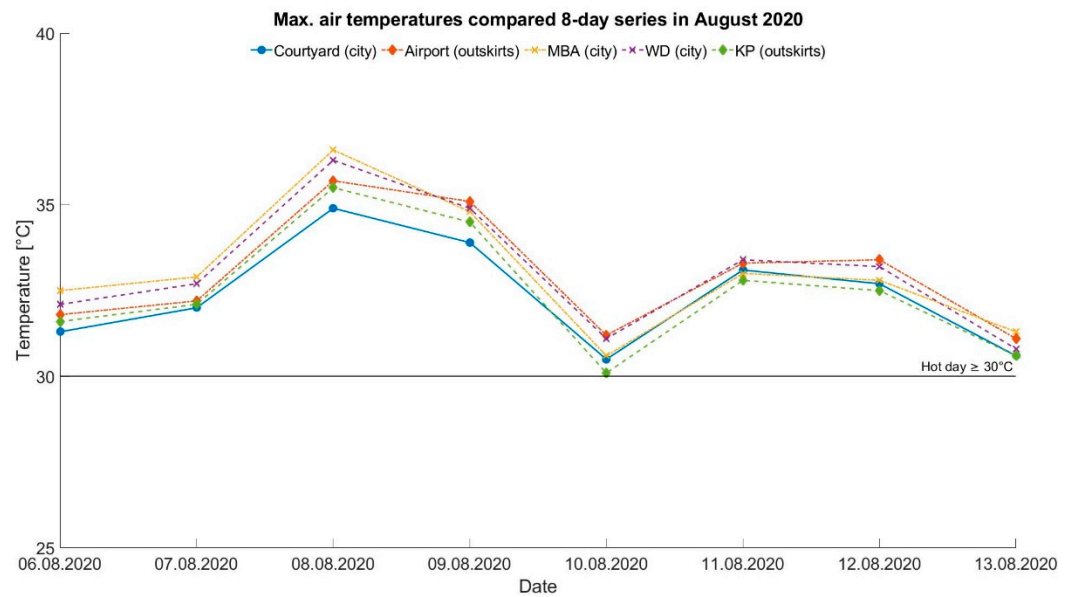
Figure 6. Heat wave in August 2020. Maximum air temperatures per day from 6–13 August. Comparison of the DWD weather stations at airport, Marianne-Baecker-Allee (MBA), Weidendamm (WD), Kattenbrookspark (KP) and the TransMiT weather station in the blue courtyard. The horizontal line marks the 30 °C limit.

Table 2. Daily maximum air temperatures during the heat wave in August 2020 for each observed station.

	T [°C] Courtyard (C)	T [°C] Airport (A)	T [°C] MBA	T [°C] WD	T [°C] KP
6 August 2020	31.3	31.8	32.5	32.1	31.6
7 August 2020	32	32.2	32.9	32.7	32.1
8 August 2020	**34.9**	**35.7**	**36.6**	**36.3**	**35.5**
9 August 2020	33.9	35.1	34.8	34.9	34.5
10 August 2020	30.5	31.2	30.6	31.1	30.1
11 August 2020	33.1	33.3	33	33.4	32.8
12 August 2020	32.7	33.4	32.8	33.2	32.5
13 August 2020	30.6	31.1	31.3	30.8	30.6
MAX	**34.9**	**35.7**	**36.6**	**36.3**	**35.5**
MIN	**30.5**	**31.1**	**30.6**	**30.8**	**30.1**

Table 3. Deviation between the maximum air temperatures from the DWD stations (A, MBA, WD, KP) and the courtyard station (C) in °C.

	Δ C-A	Δ C-MBA	Δ C-WD	Δ C-KP
6 August 2020	−0.5	−1.2	−0.8	−0.3
7 August 2020	−0.2	−0.9	−0.7	−0.1
8 August 2020	−0.8	**−1.7**	**−1.4**	**−0.6**
9 August 2020	**−1.2**	−0.9	−1	**−0.6**
10 August 2020	−0.7	−0.1	−0.6	0.4
11 August 2020	−0.2	0.1	−0.3	0.3
12 August 2020	−0.7	−0.1	−0.5	0.2
13 August 2020	−0.5	−0.7	−0.2	0
MAX Δ	**−1.2**	**−1.7**	**−1.4**	**−0.6**
MIN Δ	**−0.2**	**+/−0.1**	**−0.2**	**0**

It is shown that the highest difference in air temperatures with 1.7 °C is recorded on 8 August 2020 between the courtyard station and Marianne-Baecker-Allee. The second highest difference is on 9 August 2020 between the courtyard station and the airport

station with 1.2 °C. Both days are also the ones with the highest air temperatures in whole Hannover throughout the year 2020. To make sure that the differences do not result from measurement uncertainties of the courtyard station, Table A1 (see Appendix A) lists the uncertainties of the used sensors. For the air temperature there is an accuracy given by the manufacturer of ±0.1 °C (from 0 to 60 °C) and ±0.2 °C (from −40 to 0 °C).

Figure 7 shows the maximum air temperatures (maximum value of each 10-min period) for 8 August 2020 from 00:00 to 24:00 (UTC), as the highest temperatures of the year were measured here. It is shown that the air temperatures of the courtyard are the lowest for the most part between sunrise and sunset. During nighttime, the courtyard temperatures are higher than those of KP and airport, but lower than those of WD and MBA, which matches with the results in Section 3.3. Between 17:30 and sunset, it is demonstrated that the air temperatures at KP, airport and courtyard have a stronger decrease and therefore lower faster than those at WD and MBA.
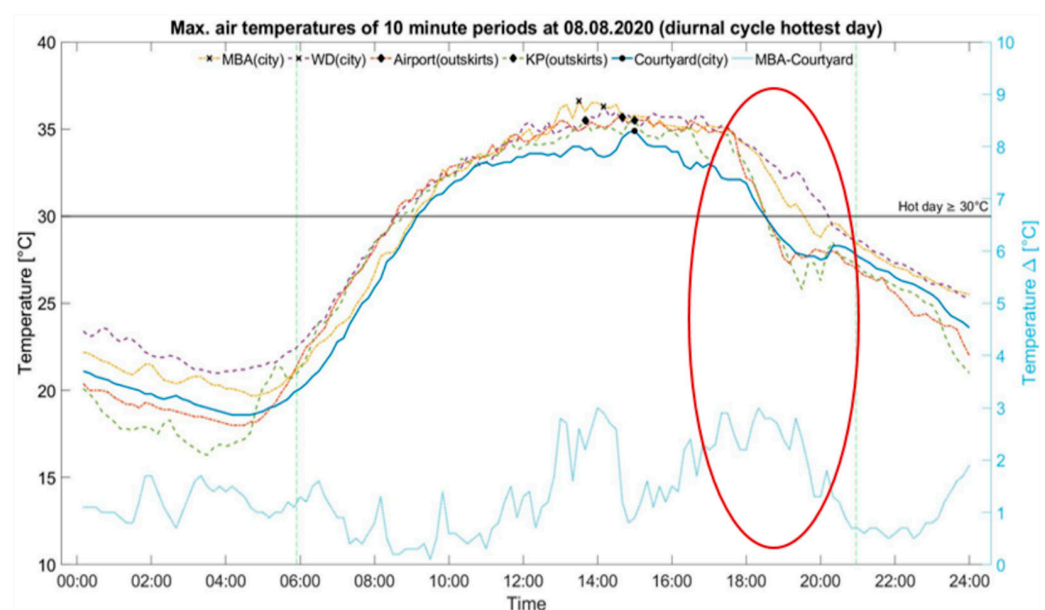

Figure 7. Maximum air temperatures of 10-min periods from 8 August 2020 (hottest day in Hannover) for the DWD weather stations at airport, Marianne-Baecker-Allee (MBA), Weidendamm (WD), Kattenbrookspark (KP) and the TransMiT weather station in the main courtyard. The horizontal line marks the 30 °C limit. The dotted vertical lines mark sunrise and sunset. The black symbols mark the maximum temperature for each station. The lower graph shows the difference between the maximum temperatures of the courtyard and the MBA station on the y-axis.

The light blue graph (referred to the second y-axis on the right) shows the difference of the maximum temperatures of the MBA station to the courtyard station. It is shown that the highest difference is 3 °C at 2 p.m. MBA was chosen due to its comparability to the courtyard area (Südstadt) regarding dense building and sealed areas in the inner city.

3.2. Tropical Nights

A tropical night is defined as "[. . .] a night in which the minimum air temperature is ≥20 °C" [31], measured from 18 UTC to 06 UTC. Following this definition, the minima of the last 10 min of each hour were used for data analysis.

Figure 8 shows the minimum temperatures per day from 1 June 2020 to 30 September 2020 for each observation station.
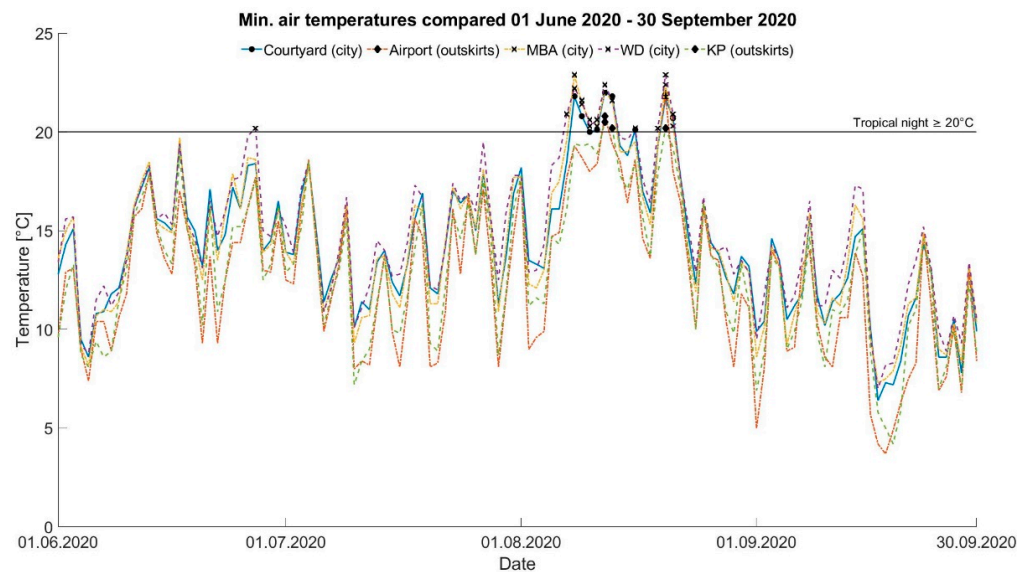
Min. air temperatures compared 01 June 2020 - 30 September 2020

Figure 8. Minimum air temperatures of the last 10 min from 1 June 2020 to 30 September 2020 for the DWD weather stations at airport, Marianne-Baecker-Allee (MBA), Weidendamm (WD), Kattenbrookspark (LP) and the TransMiT weather station in the blue courtyard. The horizontal line marks the 20 °C limit.

It is shown that there was a series of tropical nights between the 9–14 August for the stations WD, MBA and courtyard that is also shown in detail in Figure 9. It is noticeable that during this period, the stations KP and airport did only register minimum temperatures above 20 °C at 13 August and 14 August respectively. WD is the only station that measured temperatures above 20 °C during night at 28 June.
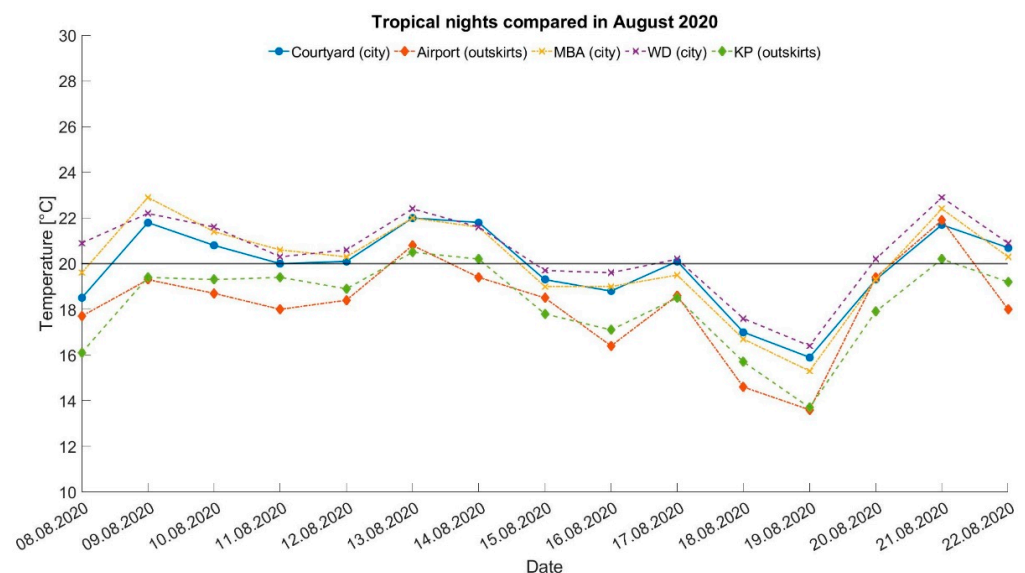
Tropical nights compared in August 2020

Figure 9. Tropical nights compared in August 2020 for the DWD weather stations at airport, Marianne-Baecker-Allee (MBA), Weidendamm (WD), Kattenbrookspark (LP) and the TransMiT weather station in the blue courtyard. The horizontal line marks the 20 °C limit.

Comparing Tables 2 and 4 (maximum temperatures) as well as Tables 3 and 5 (minimum temperatures), it becomes visible that the air temperatures between the observed stations are much more similar for the maximum temperatures during the day than the minimum air temperatures during night, especially the differences between DWD stations and the courtyard. Similar results have been obtained by [32], who also emphasize the dif-

ferences between inner city temperatures and more rural temperatures during night times, explaining that the heat island effect is a nocturnal phenomenon and is more pronounced the more built-up or sealed areas are nearby.

Table 4. Daily minimum air temperatures tropical nights series in August 2020 for each observation station.

	T [°C] Courtyard (C)	T [°C] Airport (A)	T [°C] MBA	T [°C] WD	T [°C] KP
8 August 2020	18.5	17.7	19.6	20.9	16.1
9 August 2020	21.8	19.3	**22.9**	22.2	19.4
10 August 2020	20.8	18.7	21.4	21.6	19.3
11 August 2020	20	18	20.6	20.3	19.4
12 August 2020	20.1	18.4	20.3	20.6	18.9
13 August 2020	**22**	20.8	22	22.4	**20.5**
14 August 2020	21.8	19.4	21.6	21.6	20.2
15 August 2020	19.3	18.5	19	19.7	17.8
16 August 2020	18.8	16.4	19	19.6	17.1
17 August 2020	20.1	18.6	19.5	20.2	18.5
18 August 2020	17	14.6	16.7	17.6	15.7
19 August 2020	15.9	13.6	15.3	16.4	13.7
20 August 2020	19.3	19.4	19.3	20.2	17.9
21 August 2020	21.7	**21.9**	22.4	**22.9**	20.2
22 August 2020	20.7	18	20.3	20.9	19.2
MAX	**22**	**21.9**	**22.9**	**22.9**	**20.5**
MIN	**15.9**	**13.6**	**15.3**	**16.4**	**13.7**

Table 5. Differences between the minimum air temperatures from the DWD stations (A, MBA, WD, KP) and the courtyard station (C) in °C.

	Δ C-A	Δ C-MBA	Δ C-WD	Δ C-KP
8 August 2020	0.8	−1.1	−2.4	2.4
9 August 2020	2.5	−1.1	−0.4	2.4
10 August 2020	2.1	−0.6	−0.8	1.5
11 August 2020	2	−0.6	−0.3	0.6
12 August 2020	1.7	−0.2	−0.5	1.2
13 August 2020	1.2	0	−0.4	1.5
14 August 2020	2.4	0.2	0.2	1.6
15 August 2020	0.8	0.3	−0.4	1.5
16 August 2020	2.4	−0.2	−0.8	1.7
17 August 2020	1.5	0.6	−0.1	1.6
18 August 2020	2.4	0.3	−0.6	1.3
19 August 2020	2.3	0.6	−0.5	2.2
20 August 2020	−0.1	0	−0.9	1.4
21 August 2020	−0.2	−0.7	−1.2	1.5
22 August 2020	**2.7**	0.4	−0.2	1.5
MAX Δ	**2.7**	**−1.1**	**−2.4**	**2.4**
MIN Δ	**−0.1**	**0**	**−0.1**	**0.6**

The highest difference for the minimum temperatures occurs on 22 August between courtyard and airport with 2.7 °C. The highest minimum temperatures were registered at MBA and WD on different days, respectively for MBA at 9 August and for WD at 21 August. The following Figures 10 and 11 show the temperatures of the two warmest nights registered in 2020 in comparison for each observed station. In Figure 10 it can be seen that in the night from 8 to 9 August no tropical night is recorded at KP (19.4 °C) and airport as the temperatures fall below 20 °C, although the temperatures are close to those of the other stations passing the limit temperature of the definition. Figure 11 shows the situation for 20 and 21 August when all stations registered a tropical night. The difference between the lowest temperature at KP on the night of 9 August and 21 August is 0.8 °C.
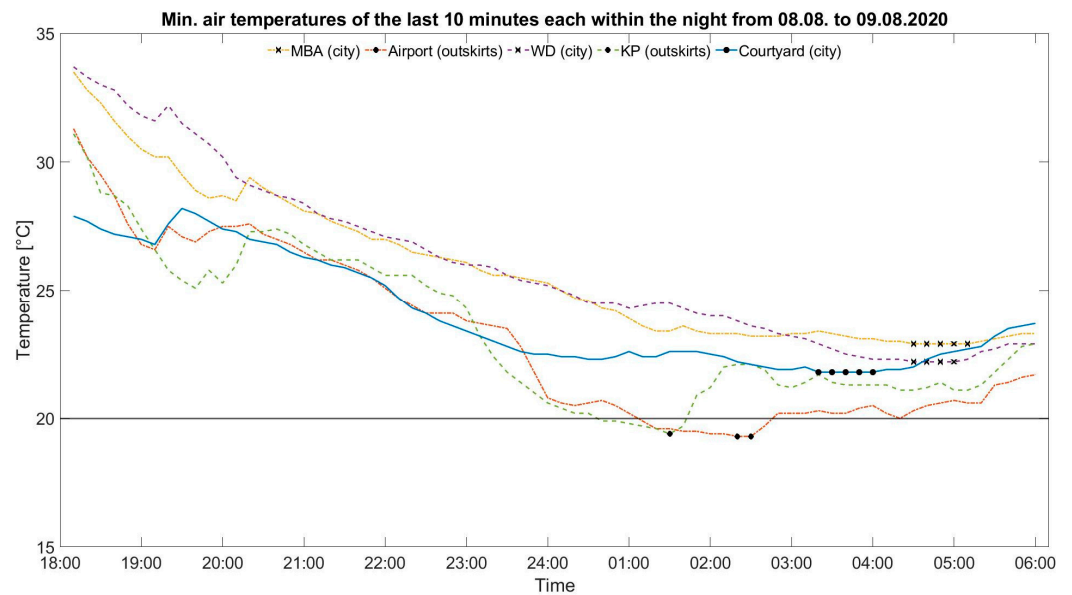
Min. air temperatures of the last 10 minutes each within the night from 08.08. to 09.08.2020

Figure 10. Minimum air temperatures of the last 10 min each within the night from 8 August to 9 August 2020. The horizontal black line marks 20 °C. The black stars mark the minimum temperatures for each station.
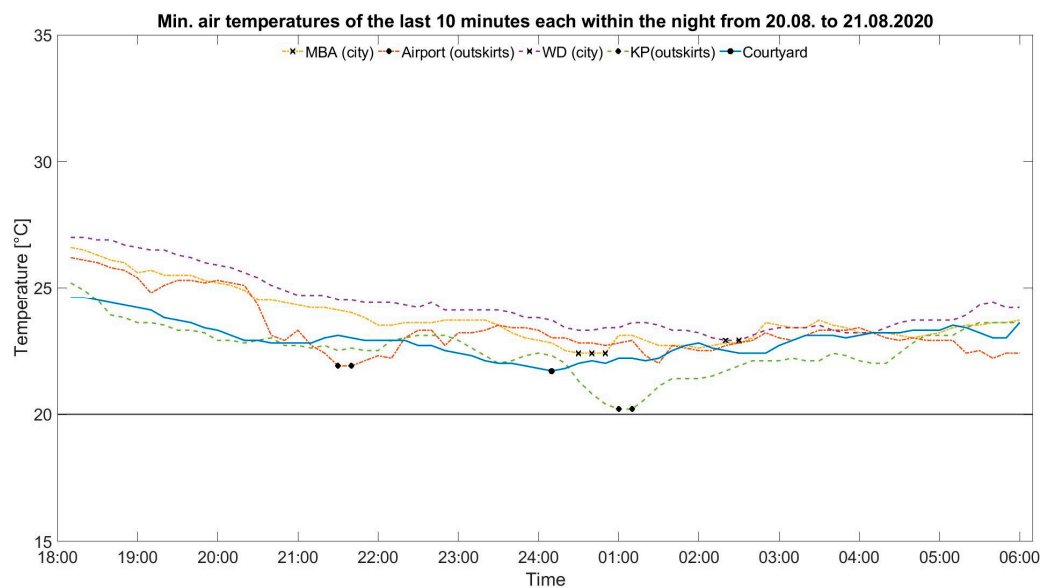
Min. air temperatures of the last 10 minutes each within the night from 20.08. to 21.08.2020

Figure 11. Minimum air temperatures of the last 10 min each within the night from 20 August to 21 August 2020. The horizontal black line marks 20 °C. The black stars mark the minimum temperatures for each station.

3.3. Tropical Nights and Hot Days in Comparison

Figure 12 compares the number of hot days and tropical nights for the different observation points. It is shown that the courtyard has the smallest number of hot days but a comparatively high number of tropical nights as these exceed the numbers of airport, KP and MBA. Only the WD station shows more tropical nights. Moreover, the difference between the number of tropical nights and hot days is comparable between courtyard and WD, while the differences for airport, MBA and KP are much higher. In average, there were 11.7 hot days and 6.8 tropical nights. For comparison: there were 11.4 hot days in average (cf. [33]) throughout Germany.
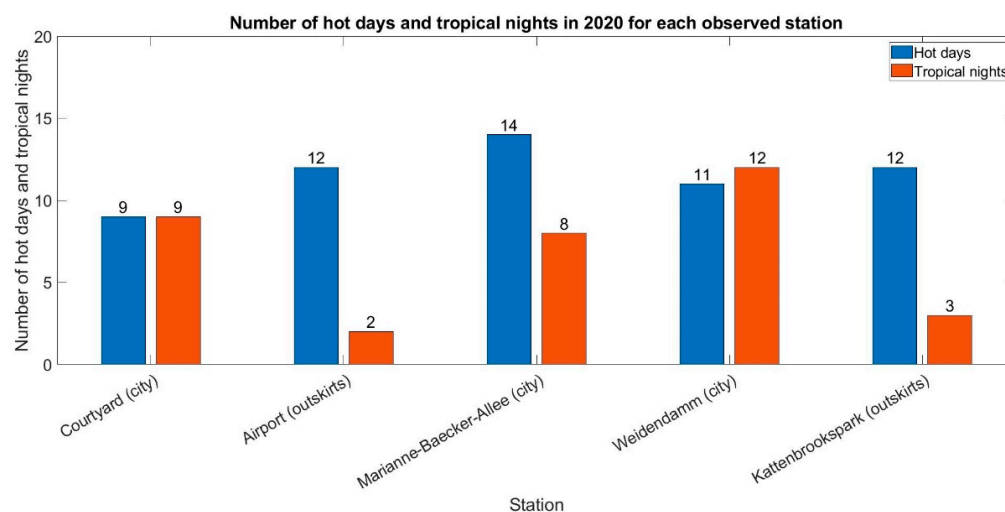
Figure 12. Number of hot days (blue) and tropical nights (red) in comparison in Hannover 2020 for mobile stations at Marianne-Baecker-Allee, Weidendamm, Kattenbrookspark as well as airport and blue courtyard.

3.4. Amplitudes

Figures 13 and 14 show the amplitudes for MBA, KP and courtyard (blue). The amplitude is the difference between the highest and lowest temperature of a certain timestep [34]. For a better overview, only three stations were evaluated (i) the blue courtyard as research focus, (ii) one city station MBA and (iii) one station of the outskirts KP. Finding the highest differences for the maximum temperatures compared to the courtyard MBA was chosen for the city station. For the outskirts station, KP was selected, because fewer external influences were assumed in comparison to the situation at the airport (e.g., influence on the wind or air exchange due to airplanes). Moreover, the KP station is located in a park—by this, a station with green surroundings and a station surrounded by asphalt is compared.
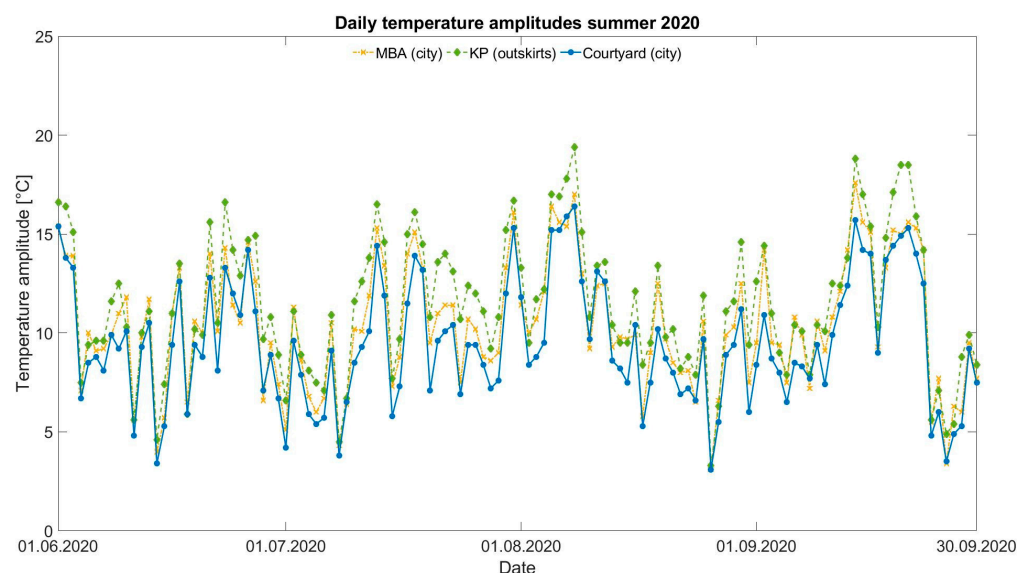

Figure 13. Daily temperature amplitudes in summer 2020 (June–September) for the stations Courtyard, Kattenbrookspark (KP) and Marianne-Baecker-Allee (MBA).
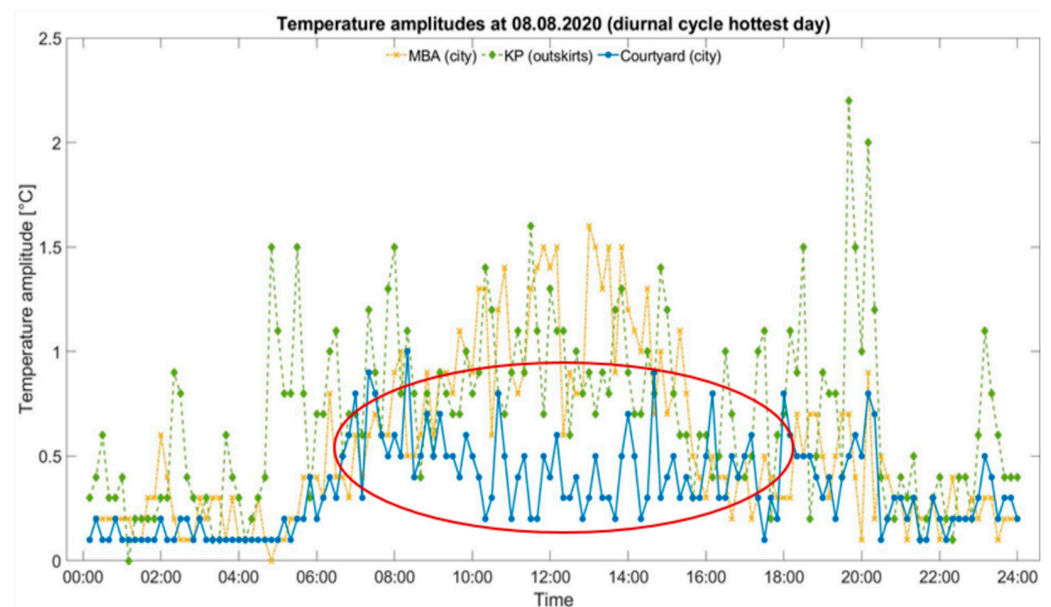
Figure 14. Temperature amplitude at 08 August 2020 for the stations Courtyard, Kattenbrookspark (KP) and Marianne-Baecker-Allee (MBA).

As seen in Figure 13, the daily temperature amplitudes from June to September of the three chosen stations have a very similar temperature curve profile. It is obvious that the curve for the courtyard is the lowest for nearly every timestep.

Figure 14 shows the temperature amplitude for the 8 August (hottest day). In this case, the amplitude was calculated using the 10-min maximum data minus the 10-min minimum data for 8 August. The diagram emphasizes that the differences between maximum and minimum temperatures for the courtyard do not vary that much as those at KP and MBA during daytime (~08:00 to 16:00). Furthermore, shows the courtyard temperature a flatter curve while the MBA amplitudes are low during night and higher around noon. The values for KP show some high peaks throughout the whole measurement period.

3.5. Drone Measurement

There are two types of results for the drone measurements at 17 June 2020 and 31 July 2020. The first part consists of the results for the vertical probing and the second part is the outcome from the infrared measurement. The results are presented separately for each courtyard in what follows.

3.5.1. Blue Courtyard (Südstadt) Measurements

Figure 15 shows the calculated potential temperature [°C], the measured temperatures [°C] and relative humidity [%] as the vertical profile for the blue courtyard. It is shown that the temperature rises from around 26.2 °C at 0 m to approximately 27.2 °C at around 18 m. With increasing height, the temperature decreases. A similar pattern (but vice versa) is demonstrated for the relative humidity. The humidity starts at 0 m with around 46%, decreases until 20 m to 42.6% and increases afterwards with height. The potential temperature shows a similar pattern. Meteorologists refer to this phenomenon of temperature reversal as an 'inversion' [35] of the temperature profile which according to [36] can follow at night after an autochthonous weather situation during daytime.
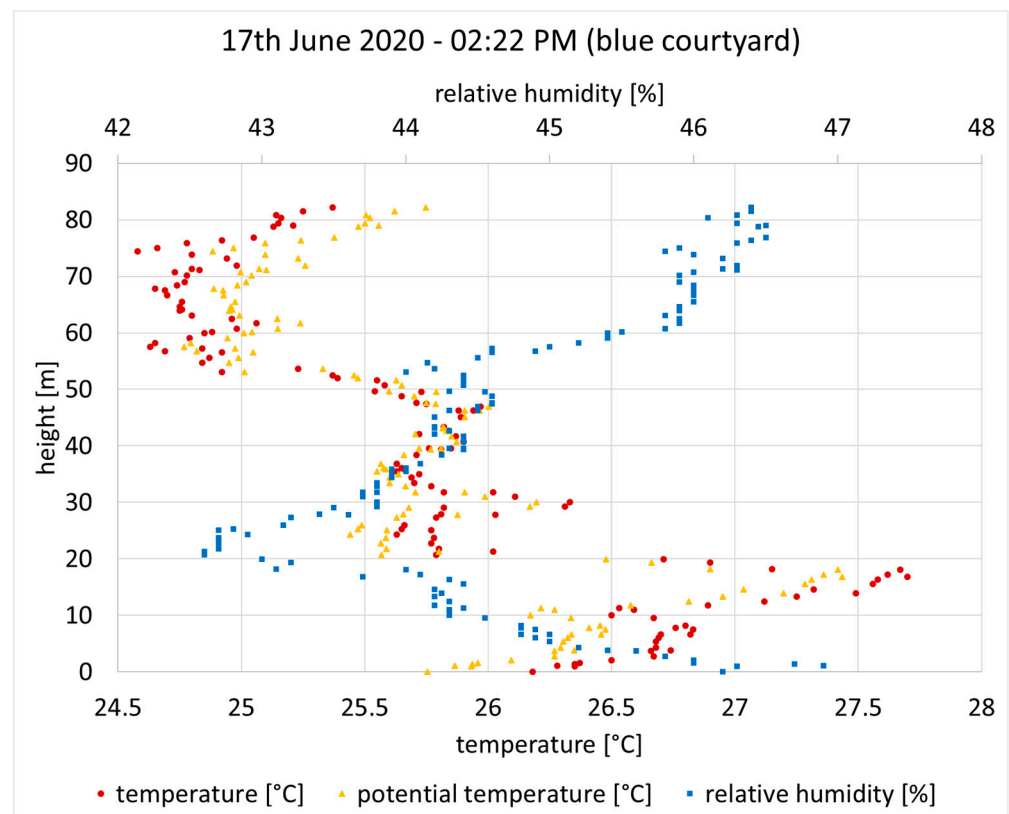
Figure 15. Results from the vertical probing (printed with permission from IMuK [37]) in the blue courtyard. The yellow dots represent the potential temperature profile, red dots represent the temperature profile and the blue dots represent the humidity profile. The lowest point (0 m) is the start, the highest point (around 80 m) the end of the measurement period. The y-axis shows the height [m], the x-axis shows the temperature [°C].

In Figure 16, the aerial (a) and the infrared image (b) of the blue courtyard are placed side by side showing that the roofs have a very high surface temperature around 50 °C, while the temperatures of the surfaces in the courtyard vary between 22 °C and 28 °C. The nearby street shows a surface temperature of around 40 °C. The shadowed areas in the backyard have the lowest temperatures while those surfaces located in the sun have higher temperatures with slightly lower average temperature inside the backyard compared to the street in front of the city block.
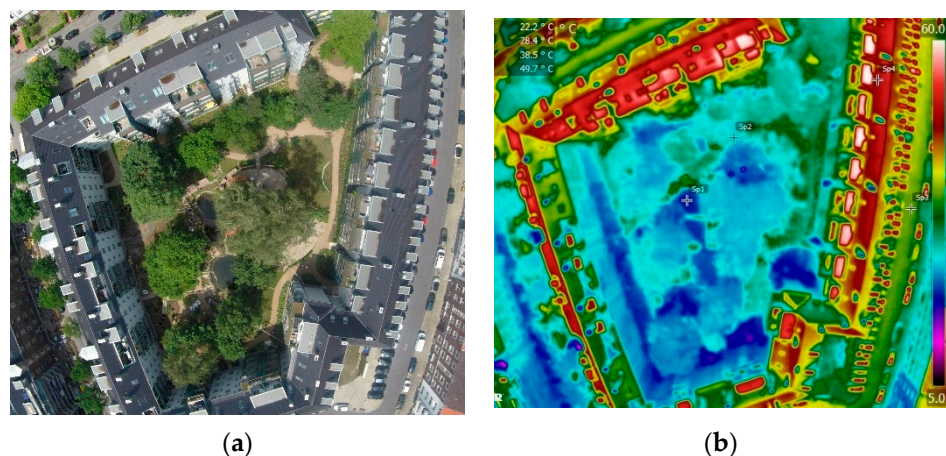

Figure 16. Comparison between aerial view (**a**) and infrared image (**b**) of the blue courtyard (printed with permission from IMuK [37]).

3.5.2. Green Courtyard (Linden) Drone Measurements

Figure 17 shows the calculated potential temperature [°C], the measured temperatures [°C] and relative humidity [%] as the vertical profile for the green courtyard. It is shown that the potential temperature rises from around 30 °C at 0 m to approximately 27 °C at around 18 m. Up to 30 m height, the drone measured an oscillating-like temperature profile with an increase to approximately 27.4 °C. A decrease to ca. 25.8 °C up to 45 m and an increase again around 25.5° at 65 m, ending at a temperature of 25.6 °C at 70 m. The actual temperature shows a similar pattern. The relative humidity starts with around 34.7% at ground level rises to ca. 40.2% at 20 m height and to 42.8% at 80 m height. There is a small decrease measured between 20–80 m.
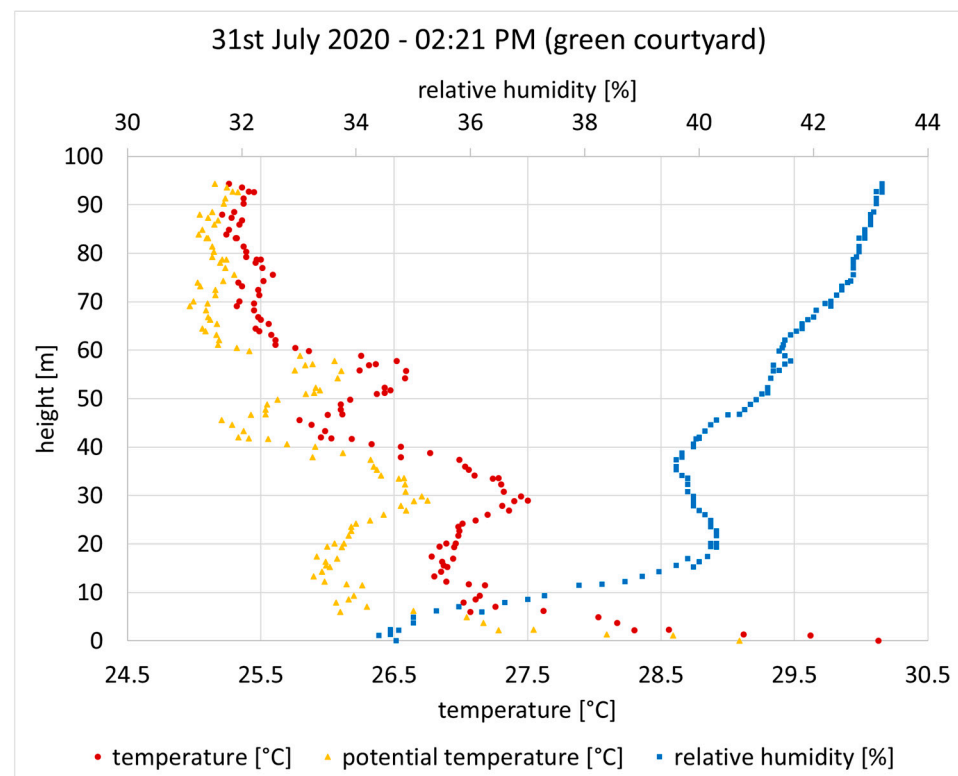

Figure 17. Results from the vertical probing (printed with permission from IMuK [37]) in the green courtyard.

The yellow dots represent the potential temperature profile, red dots represent the temperature profile and the blue dots represent the humidity profile. The lowest point (0 m) is the start, the highest point (around 80 m) the end of the measurement period. The y-axis shows the height [m], the x-axis shows the temperature [°C].

In Figure 18, again the aerial image (a) is compared to the infrared recording (b) now for the green courtyard. Similar to the blue courtyard is the basic temperature trend. The roofs have a very high surface temperature here around 68 °C, while the temperatures of the courtyard ground are lower varying between 26 °C and 42 °C. The tree surface in the middle shows a temperature of 33.6 °C and the shadowed area shows a temperature of around 26 °C. Not expected was the high temperature of the lawn area.
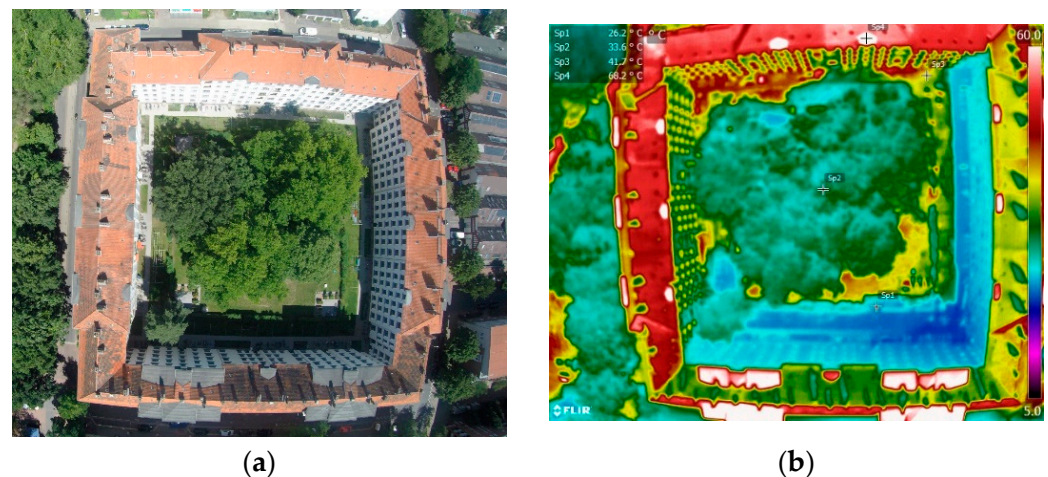
(**a**)   (**b**)

Figure 18. Comparison between aerial view (**a**) and infrared recording (**b**) of the green courtyard (printed with permission from IMuK [37]).

3.6. PALM Simulation

The leading question for conducting the simulation of the before mentioned courtyards in Hannover Südstadt is to investigate how blue and green measures, especially water bodies, affect the surrounding parts of the atmosphere. The model PALM is expected to be a promising tool to understand and quantify the effect of the measures in an urban area like the chosen courtyard.

For the analysis we picked up two points in time of the 40 simulated hours. 14:00 o'clock MEST for conditions at day and 04:00 o'clock MEST for conditions at night. The daytime was chosen after 14 h of simulation and the nighttime after 28 h of simulation, because at this time the influence of the climatic conditions of the previous day takes effect. The first night (e.g., after 4 simulated hours) was still too much characterized by the initialization and settling phase of the model.

As a preview of the simulation the surface temperature during day and night time in Figure 19 shows how differentiated this parameter in PALM reacts to the various land surface covers. During daytime, the hottest spots of about 75 °C to more than 85 °C are found on the rooftops as these surfaces are directly exposed to the sun. The lowest surface temperatures of less than 20 °C can be seen in the shaded southern parts of the courtyards. In addition, the ponds in the investigated blue courtyard show the temperature minimum during the daytime according to the temperature set based on the measurements in the input parameters. This low temperature during the day compared to the other surfaces also indicates the relief potential of the water bodies. Trees or grass areas represent relief potential as well but the real potential of trees cannot be displayed by the surface temperature as the output parameter of this quantity describes the surface temperature which is seen from above, i.e., the surface temperature of the tree crown and not of the shaded area beneath the tree.

In contrast to the day, roof surfaces represent the coolest surfaces during nighttime. The pavements act as heat sources due to their high heat capacity. The ponds in the investigated courtyard represent heat sources as well during nighttime. The effect of these warm surfaces as well as the relief promising elements on the meteorological parameters during the night will be quantified in the next step of the project.
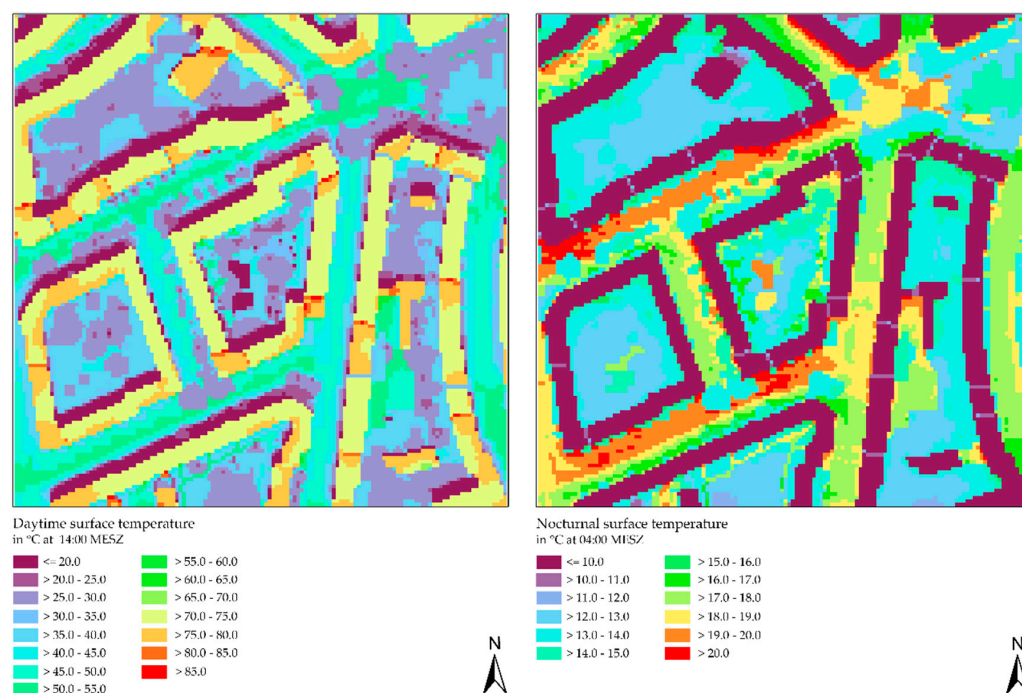
Daytime surface temperature
in °C at 14:00 MESZ

<= 20.0	> 55.0 - 60.0
> 20.0 - 25.0	> 60.0 - 65.0
> 25.0 - 30.0	> 65.0 - 70.0
> 30.0 - 35.0	> 70.0 - 75.0
> 35.0 - 40.0	> 75.0 - 80.0
> 40.0 - 45.0	> 80.0 - 85.0
> 45.0 - 50.0	> 85.0
> 50.0 - 55.0	

Nocturnal surface temperature
in °C at 04:00 MESZ

<= 10.0	> 15.0 - 16.0
> 10.0 - 11.0	> 16.0 - 17.0
> 11.0 - 12.0	> 17.0 - 18.0
> 12.0 - 13.0	> 18.0 - 19.0
> 13.0 - 14.0	> 19.0 - 20.0
> 14.0 - 15.0	> 20.0

Figure 19. Surface temperatures modelled by PALM-4U for the diverse Land surface classifications at 14:00 MESZ (**left**) and during nighttime at 04:00 MESZ (**right**).

4. Discussion

As the results show, the courtyard has as many tropical nights as hot days. However, compared to the other observed stations, the courtyard has the lowest number of hot days while the stations MBA (city), airport (outskirts) and KP (outskirts) all show the same pattern, that there are more hot days than tropical nights, but with varying differences. The only station with more tropical nights than hot days is Weidendamm (city). The highest difference between the number of hot days and the number of tropical nights can be seen for the stations KP (12 against 3) and airport (12 against 2). To summarize, significantly more tropical nights can be observed for the inner city (12 and 8) than for the surrounding areas (factor 4), which is similar to the results by [32], who mention a factor of 3 (three times more tropical night than hot days were observed). A possible explanation for the variation between the measurement sites could be the different surroundings. At KP and airport, the connecting area is open and flat; there are no barriers hindering air exchange. Furthermore, there are not many reflecting surfaces. Both, MBA and WD are temperature stations in the inner city of Hanover linked to buildings in the neighborhood of the measurement point, reflecting surfaces, a lot of sealed surfaces and traffic. It is well known that sealed surfaces store heat causing higher temperatures and plants in contrast enhance evapotranspiration, decreasing air temperature during hot and dry summer days. However, this positive effect will only occur if the plants are sufficiently supplied with water. Figure 19 shows exemplarily the result of the absence of evapotranspiration caused by drought at the lawn area.

As shown in Figure 6, the courtyard's air temperature was the lowest at the two hottest days in 2020. Two potential effects play an important role. In the first place, shading has a temperature-reducing effect due to the plants and the surrounding buildings. Secondly, according to [38], longer hours of sunshine, leading to warmer temperatures, often result in a lower relative humidity. These weather conditions provoke a higher evapotranspiration of green elements. Consequently, there is a higher effect of green elements if the air is warmer and drier (this effect is considered in the simulation study).

The diurnal cycle in Figure 7 also indicates a positive effect of the courtyard's design during the day, as the temperature between sunrise and sunset is the lowest of all observed

stations. In addition, the differences in temperature in Table 2 show that the courtyard has lower maximum air temperatures as the city stations. Table A1 makes clear that these differences do not occur due to measurement uncertainties, as the delta values lie above the uncertainty values. But, it cannot be excluded that the lower courtyard temperature results due to shadowing effects of the trees and surrounding buildings in the courtyard. A more negative effect is observed during the night, as the courtyard's temperature is not the lowest anymore. In the afternoon, the positive effect is supported again. According to [11], a smaller slope, hence a slower decrease in temperature at the afternoon, is a typical characteristic of urban areas. In reverse, the courtyard does not show this characteristic, but behaves like the stations at the outskirts (KP and airport), while MBA and WD exactly show these "urban characteristics". The expected delayed maximum temperature for city centers (cf. [32]) was not observed in our studies as shown in Figure 7. All maxima occur almost at the same time.

To compare the results with data for whole Germany, it will be referred to Figure 20 from the Federal Environmental Agency (*Umweltbundesamt)* [39]. (a) shows the number of hot days for 2020, while (b) shows the number of tropical nights. For Hanover, the diagram shows 12–15 hot days and up to two tropical nights, which certainly are the values, derived from the airport station. As it can be seen in the previous chapters, there are regions in Hanover with higher amounts of tropical nights and hot days. In ref. [40] also states that the DWD does not provide raster data sets for tropical nights as for the evaluation, daily data are not sufficient, but hourly data are required. So, it can be questioned if these graphics are representative. With regard to municipal planning, using such kind of graphics could lead to wrong measurement plans as Figure 20b by the Federal Environmental Agency implicates a more positive situation than it actual is. The surrounding buildings, the water bodies (heat storage capacity) and the plant canopy can probably explain the high number of tropical nights in comparison to the average number. The surrounding buildings obstruct the air exchange, there probably is fewer wind within the courtyard. Therefore, warm air stays within the courtyard. In addition, the water bodies may serve as a heat storage during daytime and as a heat source during night. Moreover, the plant canopy probably acts as a barrier for radiation that should leave the courtyard, so it ends up in heating the air. Finally, trees are not able to transpire during nighttime [41], so they cannot help cooling down the air after the sun has set. For a better blue-green infrastructure planning, a finer measurement network should be considered to define the exact hot spots within the city.
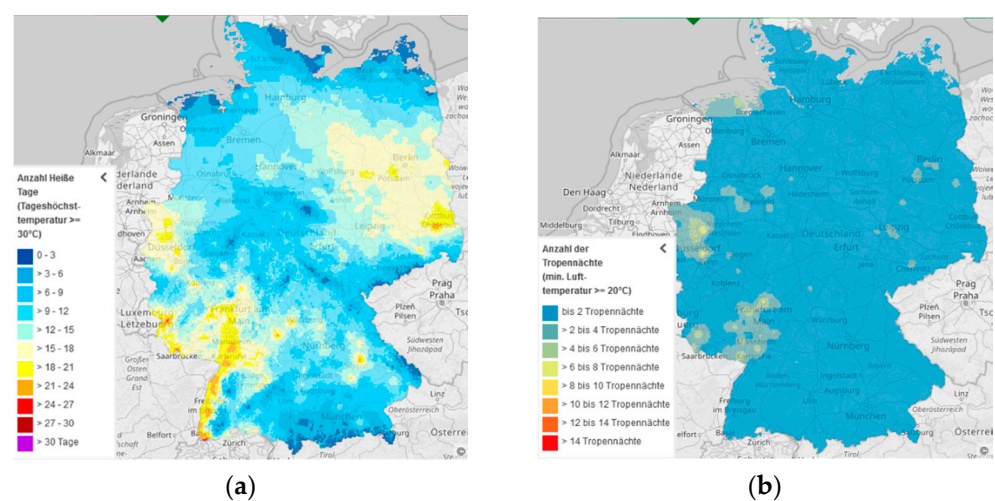

Figure 20. Hot days (**a**) and tropical nights (**b**) for Germany in 2020. Printed with permission [39].

Due to the limitations in the definition of hot days (30 °C) and tropical nights (20 °C), these indicators additionally do neglect situations that are at the margin of these limitations [22] as it is demonstrated in Figure 5 for 1 August. It is shown that for MBA one hot day is registered, but for the other stations not, although there were temperatures around

29 °C which could also lead to health burdens already [22]. Regarding this, the indicators tropical night and hot day are not enough to rate the quality of the local microclimate in the city. As an additional indicator, summer days should be considered. Summer days are days with an air temperature >25 °C [42], which would include a wider range of possibly dangerous temperature situations.

Evaluating the daily temperature amplitude, it is obvious that the courtyards temperature amplitude is the lowest of the three illustrated stations. This fits to our results for the number of hot days and tropical nights, as the amplitude shows the differences between maximum and minimum temperatures at a certain point in time. As the courtyard is located in the inner city, the statement also fits to literature—according to [11], a smaller amplitude during the day would occur for city centers (cf. [32]). Hence, a positive effect by means of the amplitude can be linked to the BGI elements in the courtyard. This even gets clearer if Figure 14 is examined. Here, the courtyard's amplitude (for one day calculated with 10-min values) seems damped compared to the amplitudes of KP and MBA, where a large gap between the amplitudes is visible. Besides, a lot of peaks are visible that show the fluctuations in air temperature of several degrees Celsius. This is most probably due to turbulences in the air layer near to the ground (2 m measurement height). The air flow is more stable during night. During day, turbulences occur more often due to thermal air flows which also could lead to air temperature changes on a small local scale and within small time steps.

The results of the drone measurements also suggest a positive effect due to the implemented blue-green infrastructure elements. As presented in Section 3.3, an inversion of the temperature profile was formed in the inner courtyard during the measurements on 17 June 2020. This leads to a lower bottom-near temperature, compared to the temperature at building height, in the courtyard during autochthonous weather. This phenomenon is assumed positive for the users of the courtyard, respectively the residents in this case, as they could use the courtyard area to cool down. To make clear that this effect is caused by the implemented blue-green elements, repeated measurements were carried out within another courtyard (see Figures 17 and 18) with mostly lawn areas (which are assumed to be relatively dry, as they were not irrigated), some trees and raised garden beds. The results show that the other courtyard does not form an inversion layer.

The discussion above shows, it is not possible to quantify all the effects of BGI just by evaluating measurements. Measuring stations are representative of a certain area, but they do not provide spatially differentiated information about the influence of every single element of the BGI on the microclimate. For this it is necessary to analyze the small-scale spatial patterns. This would require a very dense measuring network or a suitable simulation tool. Against this background, PALM-4U was selected and simulations were carried out. The aim of the first simulation of the courtyard in Hannover Südstadt was to investigate whether PALM-4U is a suitable tool for further studies on the effect of BGIs in an urban environment. Like the highly differentiated surface temperatures (cf. Figure 19) indicate, PALM-4U is capable of considering different surfaces of the urban canopy layer to a physically realistic extend. Therefore, it is expected that through further studies, the effect of BGI in the courtyard can be determined with PALM-4U. However, at least one comparative simulation of the courtyard without BGI has to be carried out for the exact quantification of the measures. In addition, a parameter study of the effect of the BGI is crucial in order to be able to investigate the sole effect of the respective measure.

The evaluation of the surface temperatures modeled with PALM-4U in this study shows very clearly the effects of vegetation and water elements on the microclimatic conditions in the two courtyards. The physical behavior of the different surfaces with its own properties are obvious and recognizable. The influence of the individual structures can be quantified for each element and shows for example that the water bodies have a cooling effect during day and a warming effect during night. Since the first approach of the local climate modeling was based on the design surface of the ponds, they do not match the real water area present during the drone measurement. In particular, the shallow pond

shows only a real surface area of 86 m^2 after a longer period of drought. This deviates significantly from the estimated 140 m^2. Based on the air temperature data, the cooling effect can thus be expected even with a smaller expansion of the water element. For a more precise estimation, supplementary drone measurements with varying water levels at different weather conditions are necessary.

An advantage of the model compared to measurements is the two and three-dimensional representation of the results which allows the evaluation of the whole investigation area. In contrast, the generation of longer time series (more than a few days) involves considerable effort and high IT costs.

5. Conclusions and Outlook

The presented results show a first approach how blue-green infrastructure elements could be quantified in their effects on a smaller local neighborhood scale by measurements as well as simulations. It is shown that the local impact on the neighborhood is relevant in terms of heat stress reduction. To support the transformation process (and municipality at the strategic planning) toward a climate-adapted urban environment, it is crucial to assist the planning with applicable tools to select the most suitable measures on a local level. Standard indicators such as the number of tropical nights and hot days are not sufficient for the evaluation of effects in small areas like courtyards or squares. These indicators are well suited for identifying hot spots, but are not yet differentiated enough for quantifying specific heat stress of urban residents. Here, effects such as local variations also play an important role and must be calculated additionally. To quantify and evaluate the effects of blue-green infrastructures it is suggested to consider summer days additionally. Other parameters like 95th and 99th percentile could be used instead of fixed thresholds (cf. [41]) to observe if there is a large difference observable in a local scale. Additionally, parameters describing surface properties like albedo, heat capacity or heat conductivity are not considered yet. They have an important impact on the specific heat stress and are influenced directly by building-related and individual measures such as facade greening, fountains, trees and so on. Especially the consideration over the entire course of the year should play a stronger role in the evaluation of the elements and urban design. As stated in [41] "urban cool island effects" due to shading and transpiration of leaf canopies may occur. These effects can only be studied by an annual observation differentiating the beginning and end of growth season. Overall, the results show that it is essential for local measurement planning, to include a finer measurement network, as the temperatures can vary significantly between different city districts. To confirm the effect of inversions within courtyards, additional drone measurements would be reasonable.

For scenario analysis and enhanced process understanding model simulations are a useful tool showing the effects of blue-green infrastructures on the microclimate. In addition to the analysis of existing structures, they offer the possibility of quantifying the effects of planned measures that have not yet been implemented. PALM-4U is a complex and powerful tool for analyzing the microclimate in urban areas. PALM-4U is suitable for the assessment and analysis of BGI, as structures such as buildings and vegetation are explicitly resolved and the energy balance of their surfaces is also calculated. As the results show (cf. Figure 19), PALM-4U is also able to calculate the energy balance and surface temperature of the different ground surfaces. This enables the realistic mapping of exchange processes in the urban boundary layer.

The resolution for investigating the effect of the BGIs was used because, on the one hand, it was considered sufficient to resolve the relevant structures in the inner courtyard and, on the other hand, it did not require too much computing time.

Nevertheless, improvements need to be made. A complete energy balance of water bodies would allow to show the influence of these elements on the microclimate more clearly and realistically. In the blue courtyard, moreover, the water temperatures of ponds and cisterns were not included in the simulation at this point but should, as it is an important parameter however, in order to include the heat storage capacity.

Meteorological models can be used to qualitatively and quantitatively investigate the effects of different BGIs. Parameters for flow dynamics and human bioclimatic parameters, such as PET and UTCI, enable the effectiveness of individual measures or the combined effect of a portfolio of measures for heat adaptation to be classified. From previous model-based analyses, however, it can also be deduced that a well-founded assessment of measures can only be derived with a very high spatial model resolution. The higher the model resolution, the more precise the assessment and localisation of the effect of the measures can be determined via a comparison of the stock versus the planned scenario. But a higher resolution is accompanied by a higher computing effort and thus higher costs. It is questionable whether this effort can be implemented for every question on the effect of measures.

To examine the effectiveness of measures, a distinction should be made between the night-time relief effect and compensatory function during the day. For the evaluation of the quality of stay and the relief effect of the exterior, static fields of the climate parameters have been considered so far. Especially for the daytime situation, however, it is decisive how movement spaces and recreational areas are used by the residents of the neighbourhood. A high balancing capacity of a green space has only a secondary benefit if it is not used by the residents (accessibility). At the same time, it is decisive how long and frequently corresponding relief spaces are used by the residents. This deficiency can be countered by a dynamic, multi-criteria approach of an agent model. Here, a representative number of virtual agents is equipped with characteristics such as age and state of health, from which an individual limit dose for the heat load is derived. These agents then roam the neighbourhood and use the common rooms for thermal relief (=reduction of the absorbed heat load). By specifying different movement patterns (e.g., way to school, way to the public transport stop, strolling in the park), a dynamic picture for a neighbourhood-representative heat load situation can be mapped for the population cross-section. It opens up the possibility for a realistic evaluation approach for the relief effect of the BGI measures. The testing of this approach is a central part for the upcoming project phase.

However, the intensive discussion with the municipal institutions during the course of the project so far has shown that these very complex and labour-intensive model approaches are too challenging in daily planning practice. Here, simpler, quick-to-use and easy-to-interpret screening approaches are probably more effective. For this reason, a screening approach based on neural network technology is being further developed in the upcoming phases of the project on the basis of high-resolution spatial climate model runs. and measurements. This screening approach is supposed to enable a quick and efficient initial assessment of the impact of heat measures, even for inexperienced and not professional users of meteorological models.

Conflicts of Interest: The authors declare no conflict of interest.

Appendix A

The blue courtyard and adjacent comparison courtyard are located in Hannover Südstadt. The green courtyard is located in Hannover Linden. The blue courtyard has a size of 3652.10 m^2 [43], the comparison courtyard has a size of around 3696 m^2 (derived from property map [44]), and the green courtyard has a size of around 3700 m^2 (derived from Google Maps [45]). The blue and comparison courtyard are both completely surrounded by buildings without openings (see Figure A1). The green courtyard is also closed, but a gate can be opened at the southern side. The buildings of the blue courtyard have a height between 16.65 m and 18.52 m [46]. The buildings of the comparison courtyard have a height around 19 m [47] and the buildings of the green courtyard have a height of around 20 m [48]. The comparison and green courtyard only include green elements like bushes, trees and hedges, while the blue courtyard includes water elements which will be described in the following. Special elements in the comparison courtyard are a water playground and a sandy playground for children. The green courtyard includes a sandy playground in the middle as well. Since spring 2021, the blue courtyard also includes a sandy playground with a climbing scaffold. As our evaluations refer to measurements from 2020, the playground in the blue courtyard is ignored for the evaluations in this paper. The green courtyard is characterized by urban gardening elements (raised garden beds) which are placed in each corner of the courtyard and are located on a sealed underground of around 40 m^2 each.
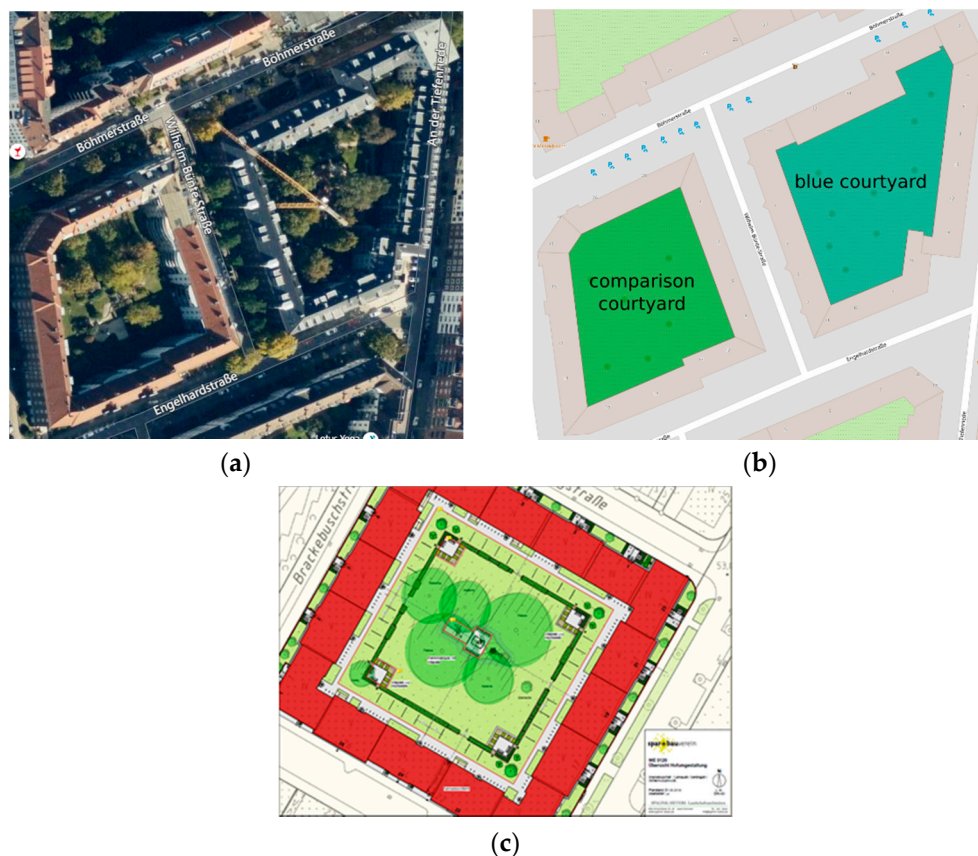

(**a**)

(**b**)

(**c**)

Figure A1. Plan views of the blue courtyard (on the right of (**a**,**b**)), the comparison courtyard (on the left of (**a**,**b**)) and the green courtyard (**c**). (**a**) Satellite view from Bing Map (© Vexcel Imaging, © TomTom, © 2022 Microsoft), (**b**) Street map from © OpenStreetMap (edited), (**c**) Plan of the green courtyard by Spar- und Bauverein [49]. Reprinted with permission from the Spar- und Bauverein [50].

The total roof area of the blue courtyard surrounding buildings amounts to 4094 m^2, while 2086 m^2 point in the direction of the courtyard and 2008 m^2 point towards the streets (due to the pitched roofs). In 2019, 449 m^2 of the roof were decoupled from the sewer system.

This corresponds to 11 % of the total roof area and 22 % of the inwards pointing roofs. The rainwater is led through rain pipes to open cisterns first (see Figure A2a). Afterwards, the water is flowing through channels and drenches to the installed ponds (see Figure A2b). The cisterns have a depth of 0.40 m and a water surface area of around 0.64 m².

(**a**)　　　　　　　　　　　　　　　　　　　　(**b**)

Figure A2. (**a**) One of the cistern cascades in the courtyard. (**b**) Channel to one of the ponds in the courtyard.

Since autumn 2020, there are three cistern cascades out of three basins each (nine basins in total). As the evaluation refer to measurements of summer 2020, the cascade system in the middle in the blue courtyard is ignored for the simulation and only the cascades in the north and south are considered in this paper.

Besides the cascade systems, there are two ponds of different depths which are called "flat pond" and "deep pond" in what follows (see Figure A3a,b). The flat pond has an estimated surface of ca. 140 m² and a maximum depth of ca. 0.40 m. The deep pond has an estimated surface of ca. 70 m² and a maximum depth of ca. 1.10 m. The ponds were filled with groundwater after completion. There is also the possibility to add groundwater when needed (e.g., if plants fall dry in summer). Both ponds as well as the channels are covered with foil, so infiltration of water is not possible. The cisterns also consist out of waterproof material.
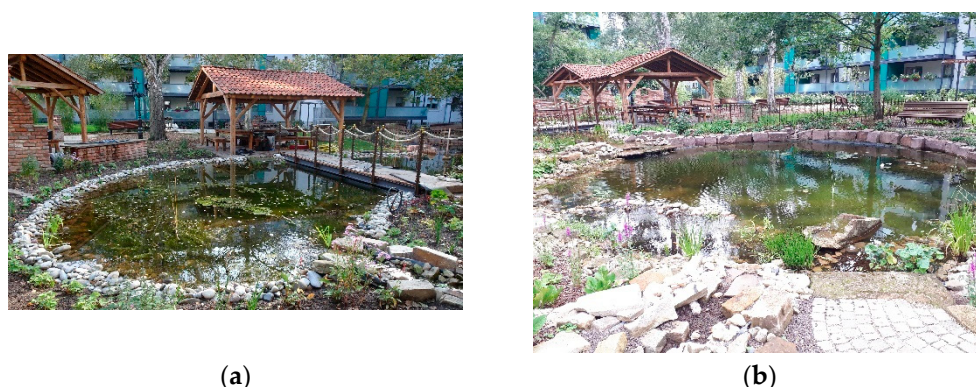

(**a**)　　　　　　　　　　　　　　　　　　　　(**b**)

Figure A3. (**a**) Flat pond—connected via water fall to deep pond. Estimated area is around 140 m², depth is around 0.40 m. (**b**) Deep pond—connected via circulation pump to flat pond. Estimated area is around 70 m², depth is around 1.1 m.

The flow scheme is shown in Figure A4. When the water level in the flat pond exceeds the height of the overflow constructed as a waterfall, the water will flow into the deep pond.

From there, water is pumped back to the flat pond with min. 8000 L/h to max. 17,500 L/h (BioTec ScreenMatic^2 140,000).
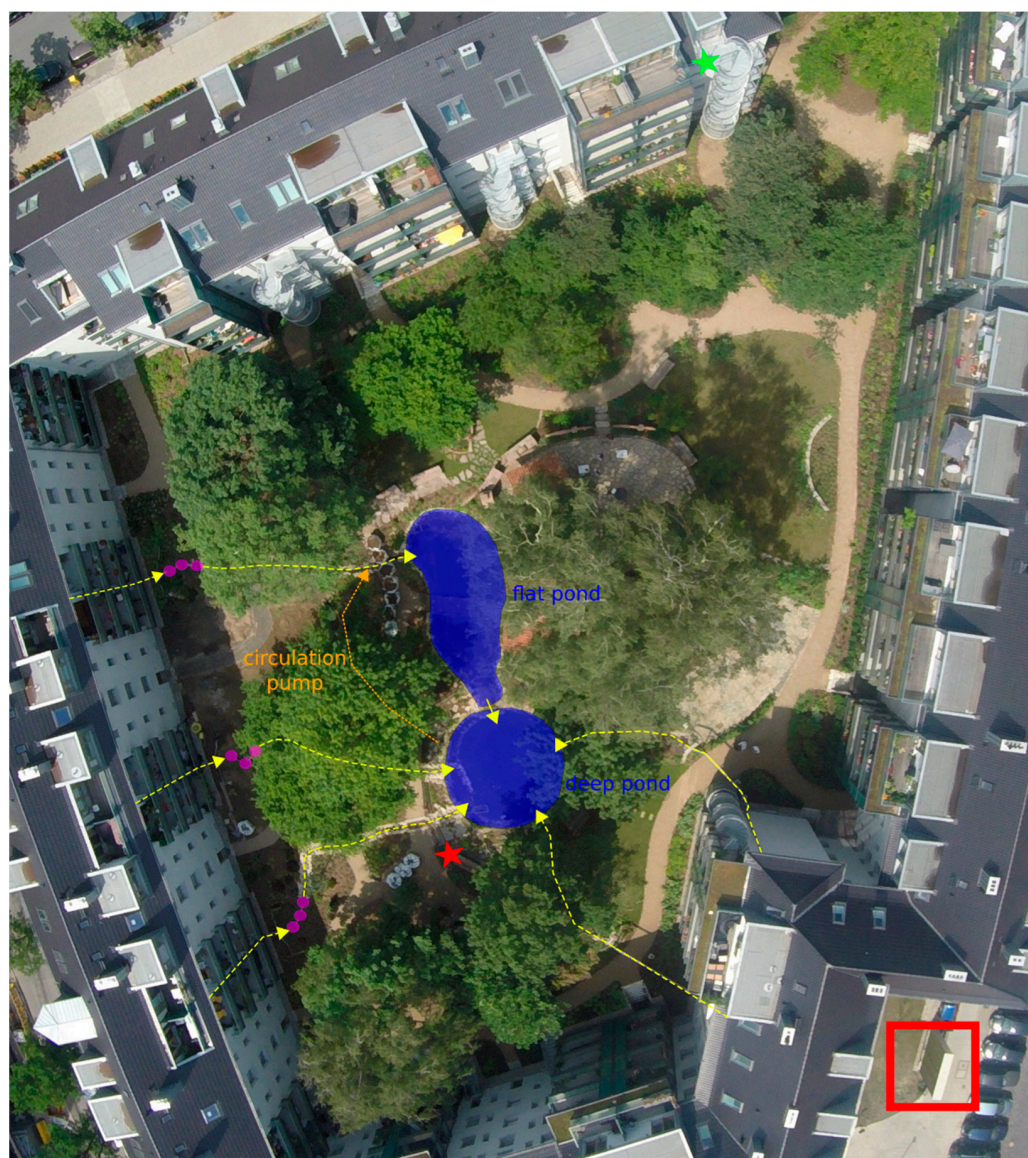

Figure A4. Plan view (by drone, printed with permission from IMuK [37]) of the water elements in the blue courtyard in Hannover Südstadt with flow scheme (not true in scale) of the rainwater from the roofs via cisterns (red dots) to the ponds (blue). The cascade system in the middle is not part of this paper as it was constructed after the measurements. The red star in the south of the deep pond marks the weather station. The green star in the north marks the pyranometer that measures global radiation. The red square in the right corner circles a moss façade near the courtyard.

Next to the deep pond is a weather station installed (red star in Figure A4). Measured parameters are air temperature, relative humidity, precipitation, air pressure (at 2 m height) and the water level in the deep pond (calculated via water pressure). Wind measurements are not carried out. In the north of the courtyard a pyranometer is installed at the top of a fire escape (green star in Figure A4).

Water temperatures are measured (i) in the flat pond, (ii) in a flat area of the deep pond, (iii) at the deepest point of the deep pond, (iv) in the middle cistern of the northern and (v) in the middle cistern of the southern cascade system. The northern cistern is located rather sunny during noon, while the southern cistern is located rather shady. Table A1

summarizes the measurement equipment used in the courtyard. All measurements started on the 28 April 2020.

Table A1. Measured parameters and measurement equipment in the blue courtyard.

Variables	Manufacturer	Equipment	Accuracy	Range	Resolution
air temperature	LAMBRECHT meteo	THP[pro] Modbus	±0.1 K (0 . . . 60 °C) and ±0.2 K (−40 . . . 0 °C)	−40 . . . +70 °C	0.1 °C
air pressure	LAMBRECHT meteo	THP[pro] Modbus	±2 hPa (at −30 . . . +70 °C) ±1 hPa (at −10 . . . +60 °C) ±0.5 hPa (at 25 °C)	500 . . . 1100 hPa	0.1 hPa
relative humidity	LAMBRECHT meteo	THP[pro] Modbus	typ. ±1.5% (0 . . . 80%) r.h. ±2% (>80%) r. h.	0 . . . 100% r. F.	0.1% r. F.
water temperature	HOBO®	Pendant® MX 2201	±0.5 °C from −20 °C to 70 °C	20 °C to 70 °C in air −20 °C to 50 °C in water	0.04 °C
precipitation	LAMBRECHT meteo	rain[e]one Modbus	0.1 mm or 2%	0.005 . . . ∞ mm (no limit)	0.001 mm (impulse outlet: 0.01 mm)
global radiation	LAMBRECHT meteo	Second Class Pyranometer, 16,103.5 series	Long-term stability <±1% change per year Non-linearity <±1% (100 to 1000 W/m^2) Directional error <±25 W/m^2 Spectral selectivity <±5% (0.35 to 1.5 × 10^{-6} m) Temperature response <±3% (−10 to +40 °C)	measurement range 0 to 2000 W/m^2 nominal operating temperature range −40 to +80 °C spectral range 285 to 3000 × 10^{-9} m	Resolution of irradiance 0.2 W/m^2

Appendix B

The following Figure A5 shows the locations of the observed weather stations (except airport and IMuK) and their location as aerial view (red stars).

According to information by [51], the DWD station at Marianne-Baecker-Allee (a,b) was surrounded on one side by nearby single buildings of varying heights, and on the other side was a wide road and a very large sealed parking lot. This measuring station had a larger area of green lawn around it.

The Weidendamm DWD station was surrounded by streets on three sides, a high single building, row development and other buildings of lower height. There was also a large intersection nearby.

The DWD station at Kattenbrookspark was located in an open area of the park, there were only bushes nearby, some single trees were further away. It is assumed that the park was not watered during summer, so the ground was probably not permanently green. There was moreover rather no shade.
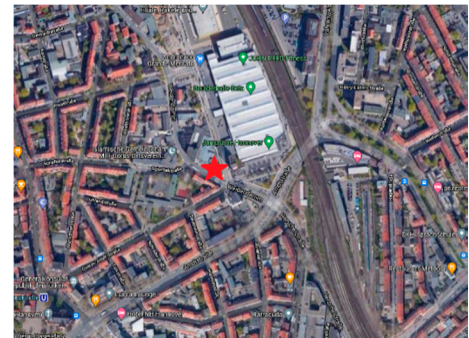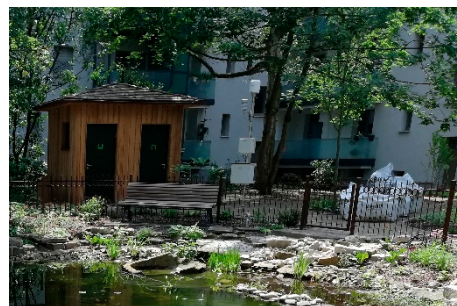
(a)
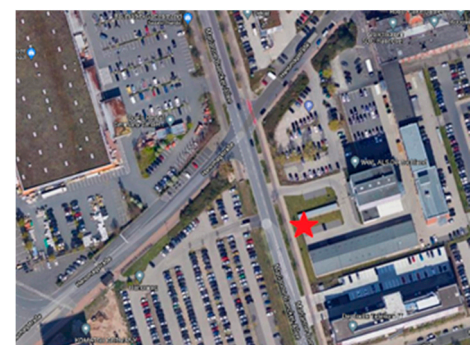
(b)

Figure A5. *Cont.*

(**c**)

(**d**)

(**e**)

(**f**)

(**g**)

(**h**)

Figure A5. Observed weather stations (except airport and IMuK) and their location as aerial view (red stars). (**a**,**b**) Marianne-Baecker-Allee, (**c**,**d**) Weidendamm, (**e**,**f**) Kattenbrookspark, (**g**,**h**) courtyard. Pictures (**a**,**c**,**e**) are provided by German Meteorological Service (DWD), Regional Climate Office Hamburg. Pictures (**b**,**d**,**f**,**h**) are Google Maps data (Map data © 2022 GeoBasis-DE/BKG © 2022, Google), usage with permission according general guidelines by Google and the fair use copyright). Picture (**g**) is by ISAH.

Appendix C

Figures A6 and A7 show the climate statistics from the Institute of Meteorology and Climatology (IMuK), representing the number of hot days and tropical nights for the period from 1951 to 2020. Both figures show an increasing trend. In 2020, there were 16 hot days and 5 tropical nights, which is comparable to the observed stations in this study.
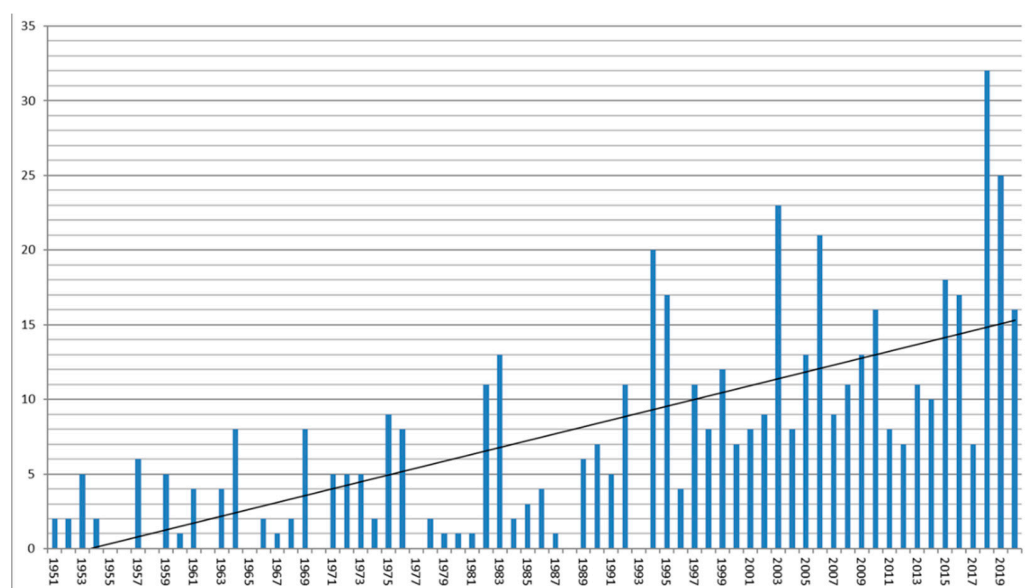
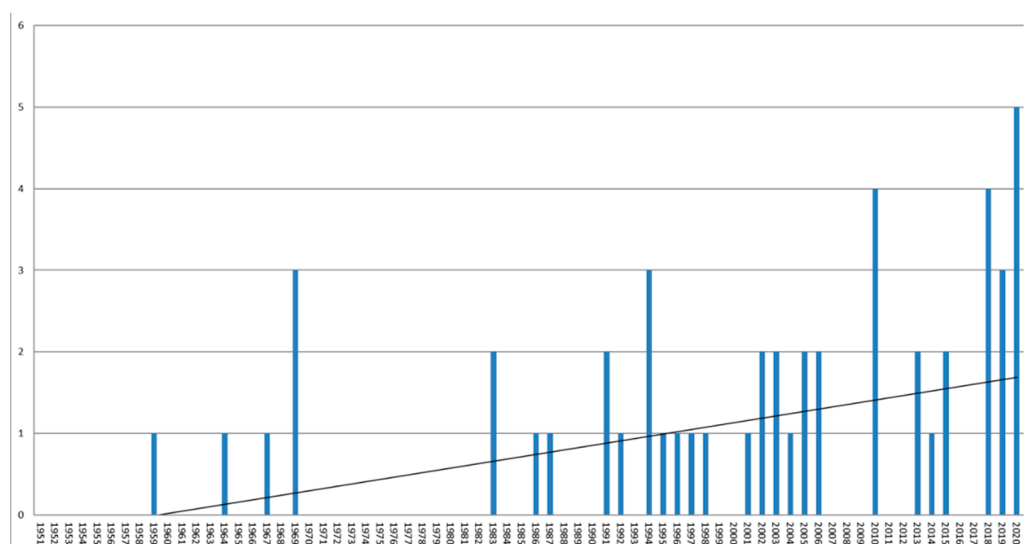**Figure A6.** Number of hot days measured at IMuK between 1951 and 2020 [52].

Figure A7. Number of tropical nights measured at IMuK between 1951 and 2020 [52].

References

1. Hajat, S.; Armstrong, B.; Baccini, M.; Biggeri, A.; Bisanti, L.; Russo, A.; Paldy, A.; Menne, B.; Kosatsky, T. Impact of high temperatures on mortality: Is there an added heat wave effect? *Epidemiology* **2006**, *17*, 632–638. [CrossRef] [PubMed]
2. Zacharias, S.; Koppe, C.; Mücke, H.-G. Climate Change Effects on Heat Waves and Future Heat Wave-Associated IHD Mortality in Germany. *Climate* **2015**, *3*, 100–117. [CrossRef]
3. German Meteorological Service (DWD). Weather and Climate Lexicon: Heat Warning. Available online: https://www.dwd.de/DE/leistungen/hitzewarnung/hitzewarnung.html (accessed on 28 October 2021).
4. Manoli, G.; Fatichi, S.; Schläpfer, M.; Yu, K.; Crowther, T.W.; Meili, N.; Burlando, P.; Katul, G.G.; Bou-Zeid, E. Magnitude of urban heat islands largely explained by climate and population. *Nature* **2019**, *573*, 55–60. [CrossRef] [PubMed]
5. Castiglia, F.R.; Wilkinson, S.J. Attenuating heat stress through green roof and green wall retrofit. *Build. Environ.* **2018**, *140*, 11–22. [CrossRef]
6. Huynen, M.M.; Martens, P.; Schram, D.; Weijenberg, M.P.; Kunst, A.E. The impact of heat waves and cold spells on mortality rates in the Dutch population. *Environ. Health Perspect.* **2001**, *109*, 463–470. [CrossRef] [PubMed]
7. An der Heiden, M.; Muthers, S.; Niemann, H.; Buchholz, U.; Grabenhenrich, L.; Matzarakis, A. Estimation of heat-related deaths in Germany between 2001 and 2015 (Schätzung hitzebedingter Todesfälle in Deutschland zwischen 2001 und 2015). *Bundesgesundheitsblatt-Gesundh. Gesundh. (Health Res.)* **2019**, *5*, 571–579. [CrossRef] [PubMed]

8. Federal Office for the Environment (Bundesamt für Umwelt/BAFU). *Heat in Cities: Basis for Climate-Adapted Urban Development (Hitze in Städten: Grundlage für Eine Klimaangepasste Stadtentwicklung)*; Federal Office for the Environment: Sachsen, Germany, 2018.

9. Patryk, A.; Świerk, D.; Krzyżaniak, M. Statistical Review of Quality Parameters of Blue-Green Infrastructure Elements Important in Mitigating the Effect of the Urban Heat Island in the Temperate Climate (C) Zone. *Int. J. Environ. Res. Public Health* **2020**, *17*, 7093.

10. Bin, Z.; Rybski, D.; Kropp, J.P. On the statistics of urban heat island intensity. *Geophys. Res. Lett.* **2013**, *40*, 5486–5491.

11. Oke, T.R. The energetic basis of the urban heat island. *Q. J. R. Meteorol. Soc.* **1982**, *108*, 1–24. [CrossRef]

12. Stewart, I.D.; Oke, T.R. Local climate zones for urban temperature studies. *Bull. Am. Meteorol. Soc.* **2012**, *93*, 1879–1900. [CrossRef]

13. Zeder, J.; Fischer, E.M. Observed extreme precipitation trends and scaling in Central Europe. *Weather Clim. Extrem.* **2020**, *29*, 100266. [CrossRef]

14. Federal Government. *German Climate Change Adaptation Strategy*; Federal Government: Berlin, Germany, 2008.

15. Merz, B.; Blöschl, G.; Vorogushyn, S.; Dottori, F.; Aerts, J.C.; Bates, P.; Bertola, M.; Kemter, M.; Kreibich, H.; Lall, U.; et al. Causes, impacts and patterns of disastrous river floods. *Nat. Rev. Earth Environ.* **2021**, *2*, 592–609. [CrossRef]

16. Reaños Tovar, M.A. Floods, flood policies and changes in welfare and inequality: Evidence from Germany. *Ecol. Econ.* **2021**, *180*, 106879. [CrossRef]

17. Bolik, I. Amphibious Urban Spaces: Integration of Decentralized Stormwater Management into Public Open Space in the Context of Climate-Adaptive Urban Redevelopment (Amphibishe Stadträume: Integration eines Dezentralen Regenwassermanagements in den Öffentlichen Freiraum im Rahmen eines Klimaadaptiven Stadtumbaus). Master's Thesis, Technical University Darmstadt, Darmstadt, Germany, 2019.

18. Senate Department for Urban Development and the Environment. *Climate Adaption for Berlin*; Senate Department for Urban Development and the Environment: Berlin, Germany, 2008.

19. City of Freiburg im Breisgau, Urban Planning Office. Climate Adaption Concept (Ein Entwicklungskonzept für das Handlungsfeld "Hitze"). 2019. Available online: https://www.freiburg.de/pb/site/Freiburg/get/params_E-1310426138/1340076/2_Klimaanpassungskonzept_Ma%C3%9Fnahmenplan.pdf (accessed on 4 November 2021).

20. Reynolds, J.S. *Courtyards. Aesthetic, Social and Thermal Delight*; John Wiley & sons Inc.: New York, NY, USA, 2002.

21. Vuckovic, M.; Kiesel, K.; Mahdavi, A. Studies in the assessment of vegetation impact in the urban context. *Energy Build.* **2017**, *145*, 331–341. [CrossRef]

22. Lower Saxony State Office for Statistics. *Statistische Berichte Niedersachsen: Bevölkerung der Gemeinden*; Lower Saxony State Office for Statistics: Hannover, Germany, 2020.

23. Statistics Office of the State Capital Hannover. The Urban Area of the State Capital Hannover in Figures. Available online: https://www.hannover.de/Leben-in-der-Region-Hannover/Politik/Wahlen-Statistik/Statistikstellen-von-Stadt-und-Region/Statistikstelle-der-Landeshauptstadt-Hannover/Hannover-kompakt/Stadtgebiet (accessed on 18 November 2021).

24. Czorny, E.; Schmidt, D.; Elsner, K.; Beier, M. Building resilience in urban neighborhoods: Reducing heat stress by integrating the water sector (German Article). *Transform. Cities* **2020**, *5*, 70–74.

25. City of Hannover. *Leben mit dem Klimawandel–Hannover Passt sich an (Living with Climate Change-Hannover Adapts)*; Landeshauptstadt Hannover: Hanover, Germany, 2017.

26. Technical University Berlin. [UC]2-Urban CLimate Under Change. Available online: http://www.uc2-program.org (accessed on 18 March 2022).

27. Maronga, B.; Banzhaf, S.; Burmeister, C.; Esch, T.; Forkel, R.; Fröhlich, D.; Fuka, V.; Gehrke, K.F.; Geletič, J.; Giersch, S.; et al. Overview of the PALM model system 6.0. *Geosci. Model Dev.* **2020**, *13*, 1335–1372. [CrossRef]

28. German Meteorological Service (DWD). Weather and Climate Lexicon: Hot Day. Available online: https://www.dwd.de/DE/service/lexikon/Functions/glossar.html?lv2=101094&lv3=101162 (accessed on 23 September 2021).

29. Steger, L.; Well, F.; Ludwig, F. Blue-green infrastructures: Transformation studies of urban open spaces using the example of Frankfurt (Blau-grüne Infrastrukturen: Transformationsstudien urbaner Freiräume am Beispiel von Frankfurt). *Transform. Cities* **2020**, *5*, 58–63.

30. German Meteorological Service (DWD). Weather and Climate Lexicon: Heat Wave. Available online: https://www.dwd.de/DE/service/lexikon/Functions/glossar.html?lv2=101094&lv3=624852 (accessed on 23 September 2021).

31. German Meteorological Service (DWD). Weather and Climate Lexicon: Tropical Night. Available online: https://www.dwd.de/DE/service/lexikon/Functions/glossar.html?nn=103346&lv2=102672&lv3=102802 (accessed on 23 September 2021).

32. Fenner, D.; Mücke, H.-G.; Scherer, D. Inner-City Air Temperature as an Indicator of Health Stress in Large Cities, Using the Example of Berlin (Innerstädtische Luttemperatur als Indikator gesundheitlicher Belastungen in Großstädten am Beispiel Berlins); Umwelt und Mensch-Informationsdienst (Environment and Man-Information Service), 2015. Available online: https://www.umweltbundesamt.de/sites/default/files/medien/378/publikationen/innerstaedtische_lufttemperatur_30-38.pdf (accessed on 30 March 2022).

33. Federal Environmental Agency (Umweltbundesamt). Indicator: Hot Days. Available online: https://www.umweltbundesamt.de/daten/umweltindikatoren/indikator-heisse-tage#die-wichtigsten-fakten (accessed on 30 March 2022).

34. Weather Lexicon (wetter.net). Amplitude. Available online: https://www.wetter.net/wetterlexikon/eintrag/amplitude (accessed on 30 March 2022).

35. German Meteorological Service (DWD). Weather and Climate Lexicon: Inversion. Available online: https://www.dwd.de/DE/service/lexikon/Functions/glossar.html?lv2=101224&lv3=101280 (accessed on 17 November 2021).

36. German Meteorological Service (DWD). Weather and Climate Lexicon: Autochthonous Weather. Available online: https://www.dwd.de/DE/service/lexikon/Functions/glossar.html?lv2=100072&lv3=100304 (accessed on 28 February 2022).

37. Meusel, G.; Institute for Meteorology and Climatology (IMuK), Hannover, Germany. Data Transfer after Drone Flight. Personal Communication, 2020.

38. Federal Environmental Agency (Umweltbundesamt). *Investigation of the Potential for the Use of Rainwater for Evaporative Cooling in Cities: Final Report*; Federal Environmental Agency (Umweltbundesamt): Dessau-Roßlau, Germany, 2019.

39. Federal Environmental Agency (Umweltbundesamt). Air Temperature Indicators: Hot Days and Tropical Nights. Available online: https://www.umweltbundesamt.de/daten/umwelt-gesundheit/gesundheitsrisiken-durch-hitze#indikatoren-der-lufttemperatur-heisse-tage-und-tropennaechte (accessed on 28 February 2022).

40. Ministry for Environment, Energy, Food and Forestry. *Answer to Question by Member of Pariament Andreas Hartenfels (BÜNDNIS 90/DIE GRÜNEN)–Printed Matter 17/14185–: Heat Days and Tropical Nights in the Year 2020*; Ministry for Environment, Energy, Food and Forestry: Berlin, Germany, 2021.

41. Fenner, D.; Meier, F.; Scherer, D.; Polze, A. Spatial and temporal air temperature variability in Berlin, Germany, during the years 2001–2010. *Urban Clim.* **2014**, *10*, 308–331. [CrossRef]

42. German Meteorological Service (DWD). Weather and Climate Dictionary: Summer Day. Available online: https://www.dwd.de/DE/service/lexikon/Functions/glossar.html?lv2=102248&lv3=102522 (accessed on 28 February 2022).

43. Architectural Office Kozjak. *Site Plan Inner Courtyard (An der Tiefenriede/Engelhardstraße/Böhmerstraße/Wilhelm-Bünte-Straße)*; Architectural Office Kozjak: Kozjak, Croatia, 2019.

44. Authority for GLL Hannover, Cadastral Office. *Hannover Real Estate Map: Parcel 25, 01390/429*; Surveying and Cadastral Administration of Lower Saxony: Hannover, Germany, 2009.

45. Google Maps. Courtyard Hannover-Linden Brackebuschstr./Wilhelm-Bluhmstr./Berdingstr./Leinaustr; Pictures GeoBasis-DE/BKG, GeoContent, Maxar Technologies, Map Data GeoBasis-DE/BKG; 2022. Available online: https://www.marriott.com/en-us/hotels/hajcy-courtyard-hannover-maschsee/overview/?scid=7f0ceae7-4b15-4889-ab3b-881bada3e4c6&gclid=EAIaIQobChMIk8P21I-T-AIV0tKWCh1PhAeZEAAYASAAEgKRyfD_BwE&gclsrc=aw.ds (accessed on 30 March 2022).

46. Gartenheim eG, Hannover, Germany. Information Courtyard and Building (An der Tiefenriede/Engelhardstraße/Böhmerstraße/Wilhelm-Bünte-Straße). Personal Communication. 2019. Available online: https://www.gartenheim.de/aktuelles/transmit-erste-auswertungen.html (accessed on 28 February 2022).

47. Wedemeier, M.-L.; Hannover, Germany. Information Courtyard and Building (Engelhardstraße/Mendelssohnstraße/Böhmerstraße/Wilhelm-Bünte-Straße). Personal communication, 2021.

48. Spar- und Bauverein, Hannover, Germany. Cross Sections Building Brackebuschstr./Leinaustr./Wilhelm-Blum-Str./Berdingstr. from 1926/1946. Personal communication, 2020.

49. Spalink-Sievers Landscape Architects. *Overview of Courtyard Remodeling (WE 0120): Brackebuschstr./Leinaustr./Berdingstr./Wilhelm-Bluhm-Str.*; Spar- und Bauverein: Hannover, Germany, 2018.

50. Sperling, I.; Spar- und Bauverein, Hannover, Germany. Permission Request for Reprinting the Overview of Courtyard Remodeling (WE 0120). Personal communication, 2022.

51. Krugmann, G.; German Meteorological Service (DWD), Climate Office Hamburg, Hamburg, Germany. Information Regarding the Surroundings of the Mobile DWD Stations. Personal communication, 2021.

52. Schilke, H.; Institute for Meteorology and Climatology (IMuK), Karlsruhe, Germany. Air Temperature Data from the Herrenhausen Measuring Tower and Permission of Use. Personal communication, 2021.